Strategies and Technology for Managing High-Carbon Ash

Final Technical Report:	September 1, 2000 - August 31, 2003.
Principal authors:	Robert Hurt, Brown University Eric Suuberg, Brown University John Veranth, University of Utah
Ph.D. students	Xu Chen, Brown University Indrek Külaots, Brown University
Report Issue Date:	February 13, 2004
DOE Award Number:	DE-FG26-OONT40907
Submitting Organization(s):	Brown University (R. Hurt) Division of Engineering, Box D Providence, RI 02912 University of Utah Department of Chemical and Fuels Engineering Salt Lake City, Utah

Disclaimer

ABSTRACT

The overall objective of the present project was to identify and assess strategies and solutions for the management of industry problems related to carbon in ash. Specific issues addressed included:

- the effect of parent fuel selection on ash properties and adsorptivity, including a first ever examination of the air entrainment behavior of ashes from alternative (non-coal) fuels.
- the effect of various low-NOx firing modes on ash properties and adsorptivity based on pilot-plant studies.
- the kinetics and mechanism of ash ozonation. This laboratory data has provided scientific and engineering support and underpinning for parallel process development activities. The development work on the ash ozonation process has now transitioned into a scale-up and commercialization project involving a multi-industry team and scheduled to begin in 2004.

This report describes and documents the laboratory and pilot-scale work in the above three areas done at Brown University and the University of Utah during this three-year project.

TABLE OF CONTENTS

EXECUTIVE SUMMARY

In recent studies, surfactant adsorption on carbon has been identified as a key phenomenon determining the suitability of coal combustion fly ash as a concrete additive. Here unburned carbon is a contaminant and its undesirable adsorption of surfactant from the aqueous concrete paste reduces the surfactant's ability to stabilize sub-millimeter air bubbles that help improve freeze-thaw resistance in set concrete.

This report presents the results of a three-year laboratory and pilot-scale study of various ways to manage the problem of unburned carbon. Following a general introduction, Chapter 1 shows that treating fly ash with ozone dramatically reduces its interaction with concrete surfactants and thus improves its suitability as a concrete additive. The global behavior of ash ozonation is studied for a variety of different ash samples, contact times, and ozone concentrations.

Chapter 2 continues this study with a careful examination of the underlying mechanism. It is found that ozone treatment introduces covalently-bound oxygen on the carbon surfaces, which converts their surfaces from predominantly hydrophobic to predominantly hydrophilic, so that the surface molecules can no longer displace adsorbed water and the carbon becomes "benign" in concrete pastes. This process is shown to occur without significant consumption of the carbon.

Chapter 3 presents a combined laboratory and pilot study of the effect of fuel selection (coal type, biomass cofiring) and firing conditions (conventional, low NOx, deep staging) on ash quality. Both fuel selection and firing mode are additional variables that could be exploited by utilities to manage ash problems. The results show that carbon properties do vary significantly with fuel choice and with firing conditions, so that LOI is not the only variable that influences ash quality.

Chapter 4 presents a systematic look at the foam index test commonly used to assess ash quality in industry. The foam index is designed to give information on the activity of unburned carbon, but is shown here to also be influened by mineral, ion, and pH effects. The results provide guidance for selecting a reliable procedure and suggest the adoption of a standard foam index test that would allow site-to-site comparison of results and the establishment of a national database on ash quality.

The data and analyses presented in this report point to the need for future work in certain areas. Recommendations for future work include a scale-up and demonstration project for assessing the potential of ash ozonation as a commercial beneficiation process, and extension of this work to the treatment of carbon-based mercury sorbents, whose very high surface area can lead to poor ash quality at relatively low dose levels.

INTRODUCTION

Pulverized coal combustion produces over 75 million tons of fly ash and bottom ash in the U.S. every year. The most widespread and economically attractive option for utilizing fly ash is in concrete manufacture, where the fly ash serves as a partial replacement for Portland cement. In most concrete mixtures, specialty surfactants, or "air entraining admixtures" (AEAs), are added to stabilize sub-millimeter air bubbles, which improve resistance to freeze / thaw cycles (see Fig. i). The bubbles are believed to provide excess volume to accommodate the expansion of residual water upon freezing in the set concrete. Solid carbon residues, if present in fly ash in high concentration, can adsorb these surfactants and render them unable to fulfill their intended function (see Fig. ii). As a result the stable air volume is too low or the mean bubble separation (spacing factor) is too high to impart the desired freeze/thaw resistance.

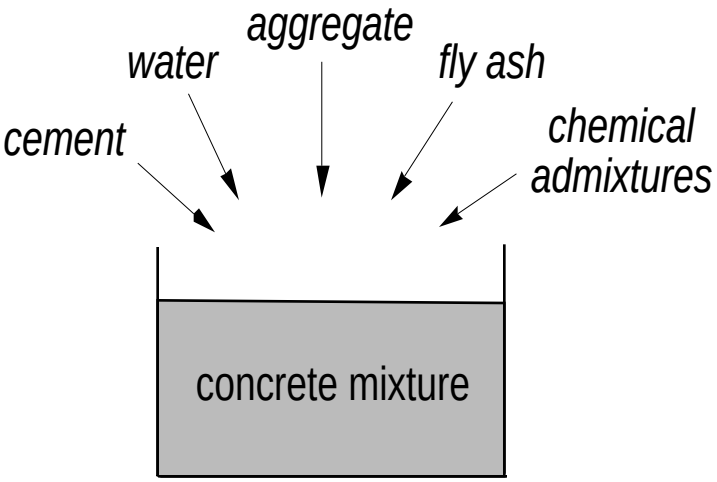

Representative structure of active surfactant in resin-derived AEA

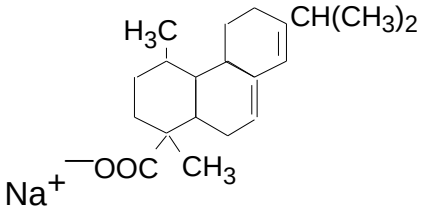

Figure i. Overview of the composition of fly ash concrete. One class of chemical admixtures are air entraining admixtures (AEA), for which a model structure is shown.

Although increasing surfactant dose may compensate for the adsorption loss, large surfactant doses in practice lead to large and intolerable variations in entrained air when normal variations in ash properties are encountered in the field. Current regulations in the U.S. limit the carbon content in ash streams for concrete applications to 2 to 6 weight-%, depending on region and regulatory body. Carbon content is typically measured by the ASTM Loss-on-Ignition (LOI) test, which reports the extent of weight loss during air oxidation at 700 ^{o}C. At high levels, carbon can discolor concrete, or lead to loss of strength, but the first problem encountered as carbon level rises is poor air entrainment behavior and this is the primary driving force for the current regulations. *If the air entrainment problem could be solved in some way, most ashes generated in the U.S. today would be utilized in concrete, even with current carbon levels.*

Almost without exception, combustion research focuses on the *amount* of char consumed and the mass of unburned carbon in ash. Recent studies, however have observed variations in the surfactant adsorptivity of commercial ash samples that cannot be explained by variations in the amount of carbon present, but are related to variations in specific carbon *properties* such as surface

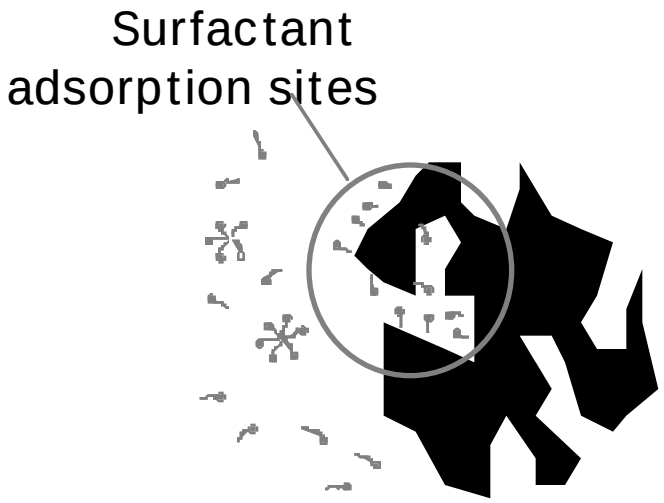

Figure ii. Surfactant adsorption on porous unburned carbon.

area, surface chemistry, and particle size. Very little is known about the effect of combustion conditions, coal type, and post-combustion treatment on carbon adsorptive properties. Several recent studies have measured the relevant adsorptive properties of commercial ash samples, but these samples come from complex and incompletely characterized combustion environments, and, as a result, it has not yet been possible to link surfactant adsorptivity to specific combustion conditions or fuel type.

A number of research and development groups are taking another approach to the carbon problem — they are developing technologies for the physical separation of carbon from the inorganic matter in ash, or for the burnout of carbon in dedicated combustion processes downstream of the boiler. These processes have not been widely adopted in the utility industry, largely due to capital cost and complexity. An alternative to these technologies is the use of ozone as described in the recent Brown University patent (US Patent 6136089). Ozonation at or near room temperature introduces oxygenated surface groups on the unburned carbon surfaces that increase the polarity of the carbon surfaces and reduce the surfactant adsorptivity, without removing significant carbon by full oxidation. In this respect the ozonation process is fundamentally different from all other proposed processes, including those in which carbon is burned out in a separate combustion process downstream of the primary coal-fired boiler. Potential advantages of ozonation include:

- simplicity of concept and operation
- operation under dry conditions, thus preserving the pozzolanic properties of ash.
- operation at ambient temperature, avoiding the need for a heat source.
- low estimated operating costs, consisting primarily of electricity.
- large-scale ozone generation is proven, off-the-shelf technology applied in water treatment, bleaching and disinfecting operations.

- ozonation does not generate a high-carbon waste stream (as do separation processes), which in most cases must be landfilled

Potential disadvantages of ozonation are:

- ozone is toxic and must be handled in sealed units (note however that ash is already handled in sealed units to prevent dust emissions)
- process leaves carbon in place, thus leaving regulatory hurdles based on LOI in some cases. Even after treatment, if the ash contains carbon above the governing local or federal limit (typically 3 or 4%), additional work is needed to verify its technical suitability for concrete, at least under current regulations.

The second cited disadvantage indicates that the most promising ash streams for initial demonstration are those that meet local LOI specifications, but still behavior poorly in concrete. We have identified a number of such field samples, typically class C ashes, and have focused early work on their treatment. It is anticipated, however, that successful with these low-carbon samples will allow even higher carbon-content ash streams to be considered in the second round of applications.

EPRI ha sbeen funding the practical development of the ozone technology, but more laboratory work was needed on the kinetics and mechanism to provide the scientific and engineering data for intelligent scale-up and optimization.

Project Objective

The overall objective of the present project was to identify and assess strategies and solutions for the management of industry problems related to carbon in ash. Options for improving or maintaining ash quality include:

- targeted fuel selection (or switching)
- modifications to combustion conditions or ash storage conditions
- post-combustion carbon surface modification by dry ozone

This project brought together a team of researchers from Brown University, the University of Utah, along with advice and consultation from Southern Company to address the problem of high carbon ash through a combination of bench scale experiments, pilot scale combustion trials with extensive analysis of collected ash samples, and the characterization of field ash samples. Specific scientific issues addressed were:

- the effect of parent fuel selection on ash properties and adsorptivity, including a first ever examination of the air entrainment behavior of ashes from alternative (non-coal) fuels.
- the effect of various low-NOx firing modes on ash properties and adsorptivity based on pilot-plant studies
- the kinetics and mechanism of ash ozonation. This laboratory data has provided scientific and engineering support and underpinning for parallel process development activities. Data from this project forms the technical basis for the scale-up and commercialization of the ash ozonation process currently being pursued by EPRI, Brown, PCI-Wedeco, F.L. Schmidt Inc., at a host site provided by PPL Generation.

DETAILED TECHNICAL DISCUSSION

This section is divided into four main chapters, dealing with (1) the global behavior during ash ozonation, (2) the detailed carbon surface chemistry responsible for the ozonation effects, (3) a combined laboratory and pilot-study of the effect of fuel selection and NOx firing mode on surfactant adsorptivity (foam index), and (4) work on the detailed mechanisms involved in the foam index test and progress toward development of an improved standard.

Chapter 1. Ash Ozonation: Global Behavior

Coal combustion fly ash is a useful additive in concrete due to its pozzolanic property — i.e. its ability to react with calcium in concrete mixes and contribute to the formation of the cementitious matrix. Through this mechanism, fly ash serves as a partial replacement for Portland cement, yielding cost savings as well as a variety of concrete property enhancements, which may include reduced permeability, improved workability, increased long-term strength, and reduced threat of long-term failure due to alkali-silica reaction [1].

A practical problem with this recycling technology is the tendency of residual carbon in ash to interfere with the air entrainment process in concrete. Porous carbon adsorbs the chemical surfactants (air entraining admixtures, or AEAs) used to generate and stabilize a micro-void system in concrete pastes [1-4]. Without a sufficient network of sub-millimeter air bubbles, concrete fails under internal pressure generated by the freezing and expansion of trapped residual water. About two-thirds of the concrete in North America is air entrained [5], and this surfactant adsorption phenomenon is the primary driving force for national and regional regulations limiting the carbon content of ash used in concrete.

Ash samples from the field show great variability in the extent to which they adsorb AEAs [2,6]. Recent work has identified the following four primary factors governing ash adsorptivity: (1) the mass fraction carbon, (2) the total surface area of the carbon [2,3,6], (3) the accessibility of that surface, as governed by particle size and pore size distribution [6,7], and (4) the carbon surface chemistry [4,6,8]. The inorganic fraction of ash is found to play a very minor role in AEA adsorption [2,6].

The role of carbon surface chemistry is particularly apparent from the behavior of ash during thermal oxidation in air. Introduction of surface oxides by exposure to air at 350 - 450 ^{o}C has been observed to significantly reduce subsequent AEA adsorption without consuming a measurable amount of carbon [8]. In contrast, treatment in inert gas at temperatures sufficient to drive-off many pre-existing surface oxides (900 ^{o}C) has been observed to *increase* adsorption [8]. Commercial carbon blacks subjected to surface oxidation processes have also been observed to be less adsorptive than non-treated varieties [3]. Both of these observations suggests that oxide-free (non-polar) carbon surfaces are the most active for adsorption of surfactants. The important role of non-polar surface is not surprising, as polar functionalities are already abundant in concrete pastes (on inorganic fly ash particles, cement particles, aggregate particles, and in the aqueous solution), whereas the only non-polar components are air bubbles and a portion of the carbon surface. The authors believe that the non-polar portions of the carbon surfaces compete directly with the air bubbles for the non-polar portions of the surfactant molecules. This insight suggests that the

deleterious effect of carbon could be suppressed by intentional oxidation of the largely non-polar carbon surfaces to introduce polar functionality.

Possibilities for intentional surface oxidation include dry and wet chemical methods. Many wet oxidation agents have been used to surface treat other carbon materials [9,10], including HNO_3, H_2O_2, CH_3COOH, and $(NH_3)_2S_2O_8$, but for the treatment of ash these wet processes would have practical disadvantages, including high drying costs, and potential problems with self-cementation or loss of pozzolanic activity. Dry oxidation in air requires temperatures above about 300 ^oC, and is not likely to offer advantages over commercial combustion-based processes, which remove the carbon altogether while operating at only modestly higher temperatures. For these reasons, the authors' efforts have focused on ozone, O_3, as an oxidant capable of attacking carbon surfaces in ash in the *dry state* and at *ambient temperature*.

There have been a number of studies of ozone reaction with various carbon materials, including graphite [11], carbon fibers [9,12,13], soot and carbon black [14,15,16], and carbon sorbents [17-19]. In these studies the applications range from the destruction of ozone waste streams (on fibers or charcoal), to the depletion of atmospheric ozone (on atmospheric soot aerosol), to surface treatment (of carbon fibers) for improved interfacial bonding in composite materials. The goal of the present short communication is to demonstrate the effectiveness of ozone for reducing the surfactant adsorptivity of fly ash carbon, and to comment on the potential for a commercial ash treatment process using the same principle.

Experimental procedures and results

Figure 1.1 shows the laboratory equipment for ash ozonation. Controlled ozone concentrations from 500 ppm - 2 vol-% were generated in air and passed upward through fixed beds of ash (50 - 200 gms), for fixed contact times (1 minute - 20 hrs), while outlet ozone concentration was monitored in real time. In these thick bed experiments, the ozone usage is typically limited by the rate of supply, and therefore the cited contact times do not reflect the true reaction kinetics, which are believed to be fast (see below). The ozonated ash samples were removed and a standard surfactant adsorptivity determined by the foam index test, a simple titration procedure used previously to quantify ash adsorptivity [2,3].

Figure 1.2A shows surfactant adsorptivity as a function of the total (integrated) amount of ozone charged for a variety of commercial ash samples and ozonation conditions (bed mass, contact time, ozone concentration). Sharp reductions are observed between 0 and 3 gm-O_3/ kg-ash. The time-resolved measurements of ozone exit concentration yield traces which vary with conditions, but

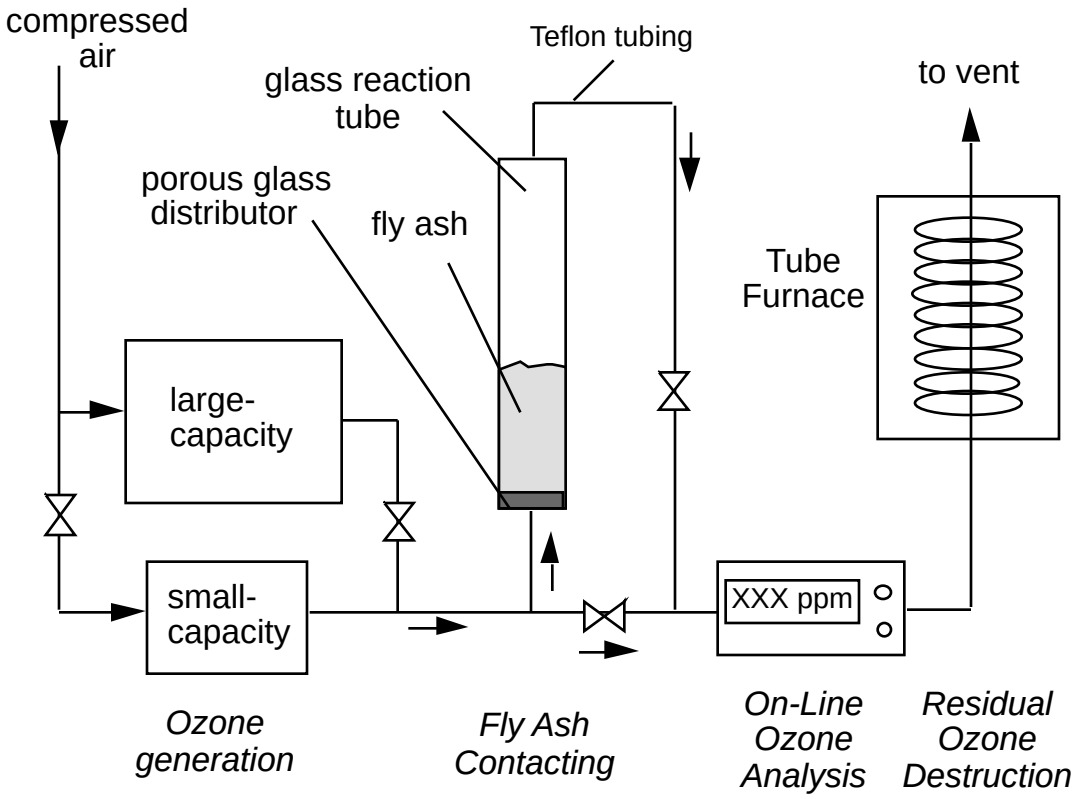

Figure 1.1 Sketch of the laboratory apparatus for ash ozonation.

typically resemble breakthrough curves in adsorber beds, exhibiting an initial period of near zero concentration followed by a rapid (though not instantaneous) rise. These traces indicate that ozone is consumed during treatment, and the curve shapes suggest relatively rapid kinetics. Based on these continuous measurement of outlet ozone concentration, a very high fraction of the charged ozone reacts within the bed for the subset of data in Fig. 1.2A lying below 3 gm-O_3/kg-ash on the abscissa. Thus the initial portion of Fig. 1.2A (0 - 3 gm-O_3/kg-ash) can be reasonably regarded as an intrinsic relation between adsorptivity and amount of ozone reacted for these ashes, while the data beyond 3 gm-O_3/kg-ash may well overstate the actual ozone requirement due to unreacted reagent loss.

Figure 1.2B shows the same data with ozone usage plotted per unit mass of *carbon*, rather than unit mass of *ash*. The carbons in class C ashes (all of which in this study derive from subbituminous coals) are seen to require more O_3 to achieve the same effect observed with class F ashes (all of which in this study derive from bituminous coals). This trend is consistent with the higher specific surface adsorptivity of carbons in most class C ashes [6]. The similar behavior of class F and C ashes in Fig. 1.2A is believed to be the fortuitous result of two offsetting effects — the class C ashes have lower carbon contents but higher specific carbon adsorptivities. Additional experiments

indicate that the reduction in adsorptivity persists during ash storage in bottles under ambient conditions for up to nine months (the longest time examined).

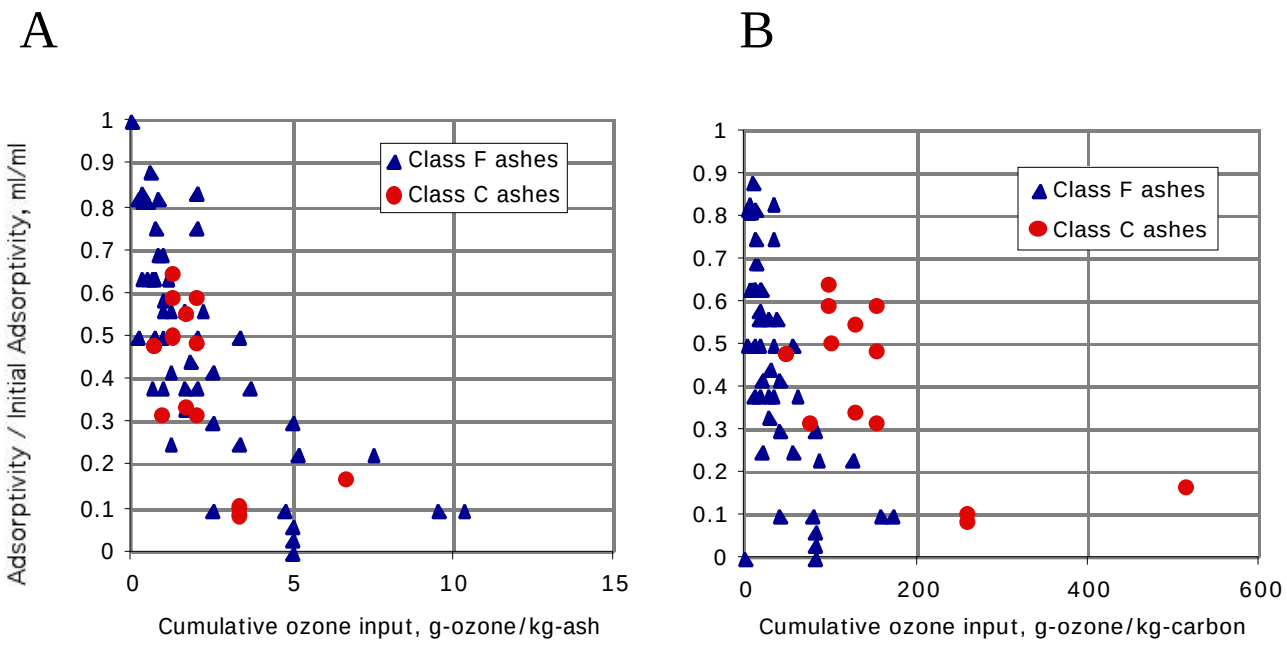

Figure 1.2 The effect of ozone treatment on surfactant adsorptivity of commercial fly ash samples. Data points represent a range of ash types, bed masses (50 - 400 gm), ozone concentrations (500 ppm - 2 vol-%), and contact times (10 - 800 min). All data are for fixed bed treatment (see Fig. 1.1) at ambient temperature and pressure. Ozone usage expressed per kg ash (panel A) and per kg carbon (panel B).

There is strong evidence that the primary mechanism of adsorptivity reduction is reactive modification of carbon surface chemistry. First, Fig. 1.3 shows that the effect is <u>not</u> related to carbon burnout, as carbon consumption is negligible in these experiments up to 20 gm-O_3/kg-ash. In fact the data suggest a slight *increase* in loss-on-ignition (LOI) presumably due to addition of chemisorbed oxygen on carbon and/or to slight mineral oxidation. Secondly, Table 1.1 shows that the reduced adsorptivity cannot be explained by reductions in <u>total</u> surface area. For ash #1, total area (by N_2 BET) is not materially affected by ozonation. Ash #2 shows significant area reduction, (similar to that observed by Deitz and Bitner during ozonation of charcoal [17,18]), but not nearly enough to explain the large decreases in surfactant adsorptivity. Thirdly, heating previously-ozonated ash samples to 1000 ^{o}C in helium for 10 minutes (a sufficient temperature to drive off most surface oxides [11]) restores most of the initial adsorptivity (see last entry in Table 1.1).

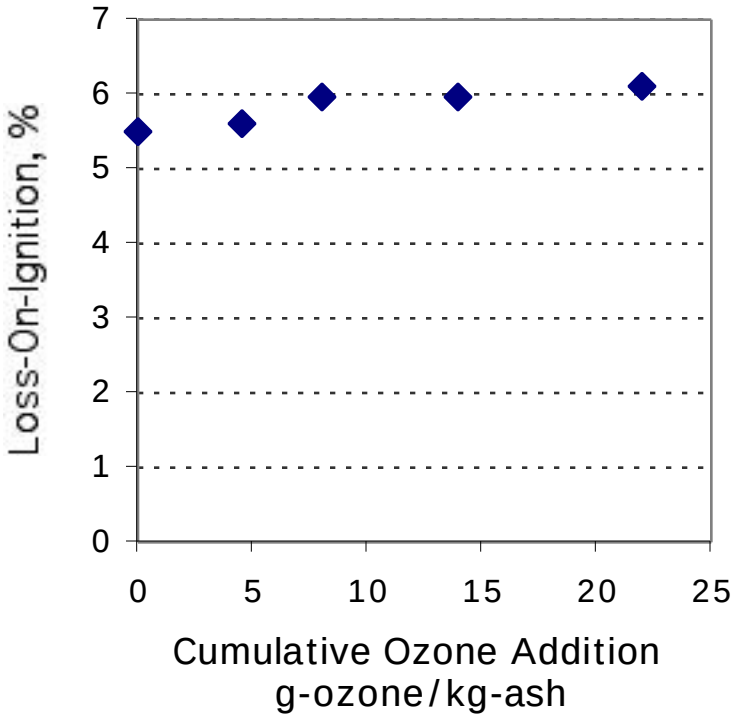

Figure 1.3 Effect of ozonation on Loss-on-Ignition (LOI), a standard test measuring fractional sample weight loss upon air oxidation at 700 ^{o}C, often used as an approximate measure of residual combustible matter in ash. Data indicate negligible carbon consumption in these experiments up to at least 20 gm-O_3/kg ash, and further suggest a slight weight gain due to the addition of chemisorbed oxygen on carbon or slight mineral oxidation.

Table 1.1 Properties of Raw and Ozonated Ashes

Ash sample	*Specific Surfactant Adsorptivity* (ml / gm-carbon)	*Carbon Surface Area (N_2 BET)* (m^2 / gm-carbon)
Ash #1, class F, from bituminous coal, 33% LOI	2.8	50.4
Ash #1 ozonated	1.0	53.4
Ash #2, class F, from bituminous coal, 6.1% LOI	3.9	51.3
Ash #2 ozonated	0.8	38.1
Ash #2 heavily ozonated	0.0	26.3
Ash #2 heavily ozonated (as above) then heated at 1000 ^{o}C in Helium	3.0	not measured

Figure 1.4 provides a final piece of evidence that surface treatment is the underlying mechanism. This plot unifies the data in Fig. 1.2B by normalizing the ozone requirement by total carbon surface area (by N_2 BET). The ozone required to achieve a given effect is directly proportional to the amount of carbon surface present. The precise reaction stoichiometry is still under investigation, but it is nevertheless useful to assume a likely stoichiometry from literature data (on other carbon materials) and to convert the abscissa in Fig. 1.4 from mol-O_3-charged/m^2-carbon-surface to an equivalent number of oxide layers on the carbon surface. The alternate abscissa at the top of Fig. 1.4 was calculated assuming one chemisorbed oxygen atom at a Van der Waals diameter of 0.28 nm, per molecule of ozone destroyed [14,19]. On this scale, the major reduction in adsorptivity is seen to occur between zero and one — i.e. during the formation of an oxide monolayer, providing a check on the reasonableness of our proposed mechanism. (Note that the data in Fig. 1.4 extend to superficial surface coverage values much greater than one. This is certainly due in part to the loss of unreacted ozone from our fixed bed reactor at long times, but may also be due to secondary chemical pathways for ozone destruction — a possibility that requires further investigation.)

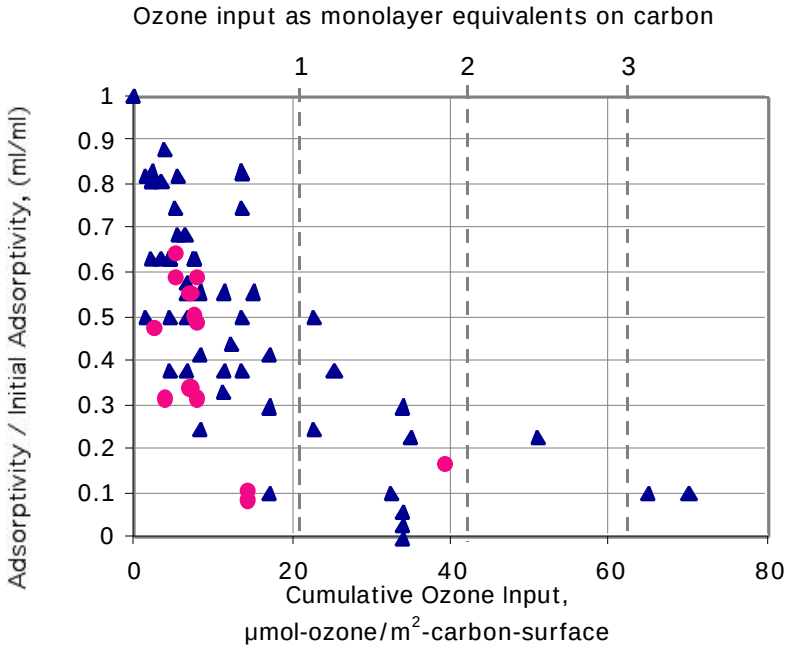

Figure 1.4 Data from Fig. 1.2 with ozone feed expressed per unit carbon surface area (by N_2 BET). Also shown is the ozone feed expressed as number of monolayer equivalents (top axis) calculated assuming one chemisorbed oxygen atom (0.28 nm Van der Waals diameter) per molecule of O_3 reacted.

The laboratory data suggest the potential for a commercial treatment process, as illustrated by the following calculation. A factor of two reduction in adsorptivity would make many currently marginal ash streams saleable for concrete application, and this level of treatment would require an ozone usage of less than 2 gm-O_3/kg-ash by the data in Fig. 1.2A. The primary cost of ozone generation is for electricity, estimated from equipment vendor data at about 7 kW-hr / lb ozone. For an electricity cost of about 0.017 $/kW-hr (utility service cost on-site [20]) these assumptions lead to an estimate of less than 0.5 $/ton ash for electrical power required for ozone generation. This cost is much less than the potential economic benefit of recovering ash salability, which is dervied from both disposal costs and sales revenues. These are region and site-specific, but can be estimated at 20 $/ton for sales in the concrete market and 30 $/ ton for disposal (1992 national average [21]). Based on these early results, fly ash ozonation warrants further investigation as a commercial alternative to physical carbon separation or carbon burnout processes.

References for Chapter 1

1. Helmuth, R. *Fly Ash in Cement and Concrete*, The Portland Cement Association, Skokie, Illinois, 1987.
2. Freeman, E., Gao, Y.M., Hurt, R.H., Suuberg, E.M. *Fuel*, 1997; 76:761-765.
3. Gao, Y.; Shim, H.; Hurt, R.H.; Suuberg, E.M.; Yang, N.Y.C. *Energy and Fuels*, 1997; 11:457-462.
4. Hill, R.L., Sarkar, S. L., Rathbone, R.F., Hower, J.C., *Cement and Concrete Research* 1997; 27:193-204.
5. Dolch, W.L., in *Concrete Admixtures Handbook, Second Addition*, (Ramachandran, Ed.), Noyes Publications, Park Ridge, New Jersey, 1995.
6. Külaots, I., Gao, Y.-M., Hurt, R.H., Suuberg, E.M., *Prepr. Am. Chem. Soc., Div. Fuel Chem*., 1998; 43:4.
7. Yu, J., Külaots, I., Sabanegh, N., Gao, Y. Hurt, R.H., Suuberg, E.M., Mehta A., *Energy and Fuels*, 2000: 14:591-596.
8. Hachmann, L., Burnett, A., Gao, Y., Hurt, R., Suuberg, E., *Twenty-Seventh Symposium (International) on Combustion*, 2965-2971, The Combustion Institute, Pittsburgh, 1998.
9. Fu, X., Lu, W., Chung, D.D.L., *Carbon*, 1998; 36:1137-1345.
10. Domingo-Garcia, M., Lopez-Garzon, F.J., Perez-Mendoza, M., *Journal of Colloid and Interface Science*, 2000; 222:233-240.
11. Magne, P., Dupont-Pavlovsky, N., *Carbon*, 1988; 26:249-255).
12. Takeuchi, Y., Itoh, T., *Sep. Technol.*, 1993; 3:168-175.
13. Rakitskaya, T.L., Bandurko, A.Y., Annan, A.A., Litvinskaya, V.V., *Kinetics and Catalysis*, 1994; 35:705-707.
14. Kamm S., Möhler, O., Naumann, K.H., Saathoff, H., Schurath, U., *Atmospheric Environment* 1999: 33:4651-4661.
15. Mul, G., Neeft, P.A., Kapteijn, F., Moulijn, J.A., *Carbon* 1998; 36:1269-1276.
16. Papirer, E., Donnet, J.-B., Schutz, A., *Carbon* 1967; 5:113-125.
17. Dietz, V.R., Bitner, J.L.,k *Carbon* 1972; 10:145-154.
18. Dietz, V.R., Bitner, J.L., *Carbon* 1973: 11:393-401.
19. Stephens, S., Rossi, M.J., Golden, D.M. *International Journal of Chemical Kinetics*, 1986; 18:1133-1149.
20. Lesky, D., Dairyland Power, personal communication, 1999.
21. Fitzgerald, H.B., Chumley, J.W., Waldrop, R.J., in *Proceedings of the Unburned Carbonaceous Material on Utility Fly ash Conference*, U.S. DOE, Pittsburgh Energy Technology Center, 1995.

Chapter 2. Ash Ozonation: Detailed Surface Chemistry

For the further development and optimization of the ash ozonation process, it is important to have a firm understanding of the underlying mechanism that gives rise to the beneficial effects. This chapter presents a comprehensive report on the mechanisms of surfactant adsorption on nonpolar, air-oxidized, and ozone-treated carbon surfaces, with emphasis on the behavior of concrete surfactants that are the origin of the problem with high-carbon fly ash utilization.

Background

Many soluble organic substances are surface active — i.e. at low bulk concentrations they exert a disproportionate influence on the interfacial and colloidal behavior of solutions. The dual hydrophobic/hydrophilic (amphiphilic) nature of surfactant molecules causes them to accumulate in interfacial regions where both the hydrophobic and hydrophilic segments can participate in favorable intermolecular interactions. Surfactants are widely exploited in industrial processes and in consumer product formulations for emulsion stabilization, foaming, detergent action, wetting enhancement, mineral separations and other purposes. Residual surfactants may interfere with downstream processing and have environmental impacts in wastewater, so there is interest in efficient technologies for their removal. Surfactant adsorption has been the subject of numerous studies [1-4], including several studies in which the sorbent is activated carbon [3,4].

In recent studies, surfactant adsorption on carbon has been identified as a key phenomenon determining the suitability of coal combustion fly ash as a concrete additive [5-9]. Here the carbon is a contaminant and its undesirable adsorption of surfactant from the aqueous concrete paste reduces the surfactant's ability to stabilize sub-millimeter air bubbles that help improve freeze-thaw resistance in set concrete [10]. Previous studies [5,7,11,12] have related the extent of adsorption to four factors: (1) the amount of residual carbon in ash, (2) the total carbon surface area, (3) the accessibility of the surface as governed by pore and particle size distribution, and (4) the state of carbon surface oxidation. Oxidation of carbon surfaces by either air or ozone has been shown to reduce the extent of concrete surfactant adsorption [7].

Intentional surface oxidation by ozone is of potential interest as an ash beneficiation process [7], so there is a motivation for developing a more fundamental understanding of its effects. The literature provides much insight into carbon surface chemistry and its role in adsorption [3,13-16] but this role depends greatly on the adsorbate and very few of these studies have examined surfactants [3,4]. A number of studies have examined carbon surface treatment with ozone [7, 13,17-26], but only our recent work has focused on its effect on surfactant adsorptivity [7]. This previous study did not yield a complete understanding on adsorption mechanism, in large part due to the complexity of the ash/surfactant system. First the abundant inorganic oxides in ash make the characterization of oxides on residual carbon surfaces difficult. Secondly, most commercial concrete surfactants are complex mixtures derived from natural sources, most commonly wood resins, and it is not possible to precisely specify the molecular structure and molecular weight of the active components from these surfactants.

The present work focuses on the mechanisms of surfactant adsorption and especially on the mechanism of its suppression by ozone treatment. This study includes detailed surface

characterization of raw and oxidized carbon black samples used as a model adsorbent with low surface polarity and few inorganic impurities. The present work also includes experiments on well-defined, single component surfactants to complement the previous studies on the multi-component commercial concrete surfactants. The results are used to discuss the driving forces for surfactant adsorption mechanisms, which are relevant both to fly ash concrete and to other situations in which amphiphilic molecules are adsorbed by carbon from the aqueous phase.

Experimental

This study focused on five carbon materials:

1. M120 carbon black (Cabot Corp., Billerica, MA) with BET area 38 m^2/gm.
2. M120 oxidized in air at 450 ^oC for 10 hrs (accompanied by 20% weight loss).
3. M120 oxidized by ozone at ambient room temperature (negligible mass loss).
4. "Ash #1": A commercial carbon-containing fly ash from bituminous coal combustion at the full scale. The fly ash is sample FA21 in the Brown University sample bank with 6.3% loss on ignition (approximately 6.3% elemental carbon), which has been used in previous studies [5,6].
5. "Ash #2": A second commercial fly ash, FA22 in Brown University sample bank, with high residual carbon level (33%).

The air oxidation was carried out in a horizontal tube furnace in a 1 lit/min flow of compressed air. Ozone treatment consisted of passing 1.5 lit/min of a 2 wt-% O_3 in O_2 mixture in upflow through a small fixed bed of sorbent. The input amount of ozone per weight of carbon black were varied to give different extents of oxidation characterized in terms of ozone dosage, g-ozone-fed/kg-carbon. Three surfactants of varying type were used in this study. Darex II (W.R. Grace, Cambridge, MA) is a commercial surfactant for air entrained concrete applications. It is a complex mixture derived from byproducts of the forest product industry. An example component is the sodium salt of abietic acid, $C_{19}H_{29}COOH$ — a three ring carboxylic acid with short aliphatic side chains found in pine resin. The sodium salt forms a globular organic anion upon dissociation in the basic aqueous medium of concrete pasts. Sodium dodecyl sulfate, $[(CH_3(CH_2)_{11}OSO_3^-][Na^+]$, or SDS is a common anionic surfactant with molecular weight 288, whose nonpolar part is an aliphatic chain, in contrast to the globular abietic acid salt. Tergitol (Aldrich Chemical) is a synthetic polyether nonionic surfactant, $CH_3(CH_2)_8(C_6H_4)(OCH_2CH_2)_9OH$, with molecular weight 616.84.

This study employs both single component surfactants (SDS, Tergitol) and a multi-component natural product that is of special technological interest for concrete (Darex II), the latter product having a complex set of components of varying surfactant activity. For this reason the extent of adsorption is characterized in this work by a titration procedure that measures amount of surfactant required to achieve stable foam in the presence of the sorbent, rather than by assay of the surfactant remaining in solution. The procedure is a modification of the "foam index" titration commonly used in the concrete industry and is described in previous publications [6]. Briefly, the test sorbent is added to 25 ml of distilled water, to which is added 8 gms of cement which provides a standard high-pH aqueous medium, and surfactant solutions are titrated in 0.02 ml per drop until stable foam appears on the surface upon agitation. A blank experiment is conducted without the test sorbent, and the required surfactant amount subtracted. The result is expressed as a "surfactant adsorptivity" in milliliters of standard surfactant solution/gram-sorbent. Alternative approaches

using direct surfactant assay by UV adsorption have been attemped [11] but fail to provide an appropriate index of adsorptivity, likely due to differences between the components with strong optical absorbance and those with high surfactant effectiveness [11]. In the experiments with single component surfactants, results will also be expressed as molar uptakes (mol surfactant / g-carbon) to aid in interpretation.

A variety of tools were used to characterize the carbon surfaces. Total oxide coverage was measured by thermal desorption using a Cahn 2141 TGA with a large sample bed (150 mg) to minimize the effects of sample consumption by trace oxygen as a fraction of total sample mass. XPS was carried out at Evans East Laboratories (East Windsor, NJ) using a Physical Electronics 5700LSci with a 350 Watt monochromatic aluminum source and an exit angle of 65º. To help understand adsorption forces, carbon black surface energies were determined by measurement of contact angles for standard liquids at the analytical laboratories of Kruss USA (Charlotte, NC). It is difficult to obtain fully dense, flat surfaces in carbon black pellets for direct measurement of contact angle, so the standard Washburn technique [27] was used in which liquids are drawn into a porous test solid and the contact angle derived from analysis of the rate of uptake relative to reference liquids that completely wet the substrate (contact angle of zero). Here hexane was used as the reference liquid and the Kruss Processor Tensiometer K12 used to measure the rate of liquid uptake gravimetrically. Water would be a natural choice for a standard liquid since hydrophilicity is of specific interest in this application, but early experiments showed water contact angles greater than 90º on the raw carbon black, and the Washburn technique is restricted to cases where $\theta < 90^o$ in which liquid uptake is spontaneous. Therefore benzyl alcohol and nitromethane were chosen as standard reference liquids, as they each wet the carbon black samples ($\theta < 90^o$) and have significantly different polarities (see Table 2.1). Knowing the surface tensions of the two standard liquids and their polar and dispersive components, the measured contact angles can be used to derive total surface energy and its polar and dispersive components by application of the Fowkes/Owens-Wendt theories as described later.

Table 2.1
Properties of standard wetting liquids and their contact angles on untreated and oxidized carbon blacks

Properties of Standard Liquids	Benzyl alcohol	Nitromethane
Surface tension, mJ/m^2	39	36.5
Dispersive component, mJ/m^2	30.3	22.0
Polar component, mJ/m^2	8.7	14.5
Polar fraction	22%	40%
Contact Angles on Carbon Blacks		
Untreated carbon black	64.4 º	68.3 º
Air oxidized at 450 ºC, 10 hrs	48.8 º	48.9 º
Treated in 2 wt-% O_3 (600 g-O_3/kg-C)	34.6 º	30.5 º

Differential scanning calorimetry was performed using a DuPont DSC 2910. 13-15mg of sample was loaded onto a non-hermetic aluminum pan after equilibration at 25 °C. The temperature was ramped at 5-25 °C/min to a final temperature of 600 °C. Prior to each set of runs, the calorimeter was calibrated with 10 mg of indium and 15 mg of zinc. FT-IR spectra of the carbon surfaces were obtained using a Nicolet Magna-IR 560 Spectrometer in transmission mode. KBr was mixed with 0.1 wt-% of the carbon test sample and milled, after which pellets were made in a laboratory press at 10 tons for 10 minutes. The pellet was dried at 90 °C for 8 hours. A set of 10 spectra was obtained for each sample. The hygroscopic nature of the carbon surfaces was examined by placing freshly prepared or freshly dried surfaces in a closed chamber with an open dish of water and the moisture uptake measured gravimetrically by drying at 110 °C for 2 hours. Surface acidity was measured using the sonic slurry method in ASTM1512-95, the standard pH test for carbon black samples. Carbon black (1.5g) was placed into a beaker with 20 ml distilled water. Several drops of acetone were added to help dispersion. After 3 minutes of agitation in an ultrasonic bath, the pH of the slurry was measured by using Corning 455 pH meter, which was calibrated by using buffers at pH of 4.0 and 10.0.

Results and discussion

Adsorption behavior

Figs 2.1-2.4 show the effects of surface oxidation on surfactant adsorptivity. Carbon black and fly ash carbon behave in similar fashion (compare Figs. 2.1 and 2.2), so the choice of carbon black as a model for fundamental surface studies is appropriate. The suppression is largely reversible upon thermal desorption of the oxides in N_2, but a significant hysteresis is also seen; the adsorptivity after 1000 °C thermal desorption ranges from 60% - 130% of the initial (pre-oxidation) value. Thermal desorption of the oxides in 1%v/v H_2/He atmosphere increased the surfactant adsorptivity relative to desorption in N_2 (Fig. 2.2). Air and ozone are both effective oxidants for adsorption suppression, and the somewhat greater effect seen for ozone in Fig. 2.2 correlates with the near-surface concentration of oxygen atoms by XPS (Fig. 2.3). Fig. 2.4 shows that the extent of suppression by ozone is similar for the three surfactant types. Overall, surfactant adsorption is strongly suppressed by surface oxidation for each of the surfactant/carbon/oxidant systems studied here.

Surface area and porosity

A possible physical mechanism of absorption suppression is the blockage of fine porosity by surface oxides [28,29]. Table 2.2 shows that ozonation does decrease the total carbon surface area for ash #1, but not by a large enough factor to explain the loss in adsorptivity. Neither ash #2 nor the carbon black decreases in surface area upon ozonation. In this respect carbon black is a useful model substance for isolating the effects of surface chemistry, because its surface area is located primarily on the external surfaces of the primary particles (75 nm in diameter) and is thus primary meso- and macro-porosity which is not easily blocked by sub-nanometer scale surface oxides. It is notable in Table 2.2 that air oxidation greatly increases carbon black surface area, presumably due to the creation of micro-porosity, but that the surfactant adsorptivity is decreased nevertheless. It is clear that the primary mechanism through which surface oxidation suppresses surfactant adsorption must be related to surface chemistry rather than pore blockage.

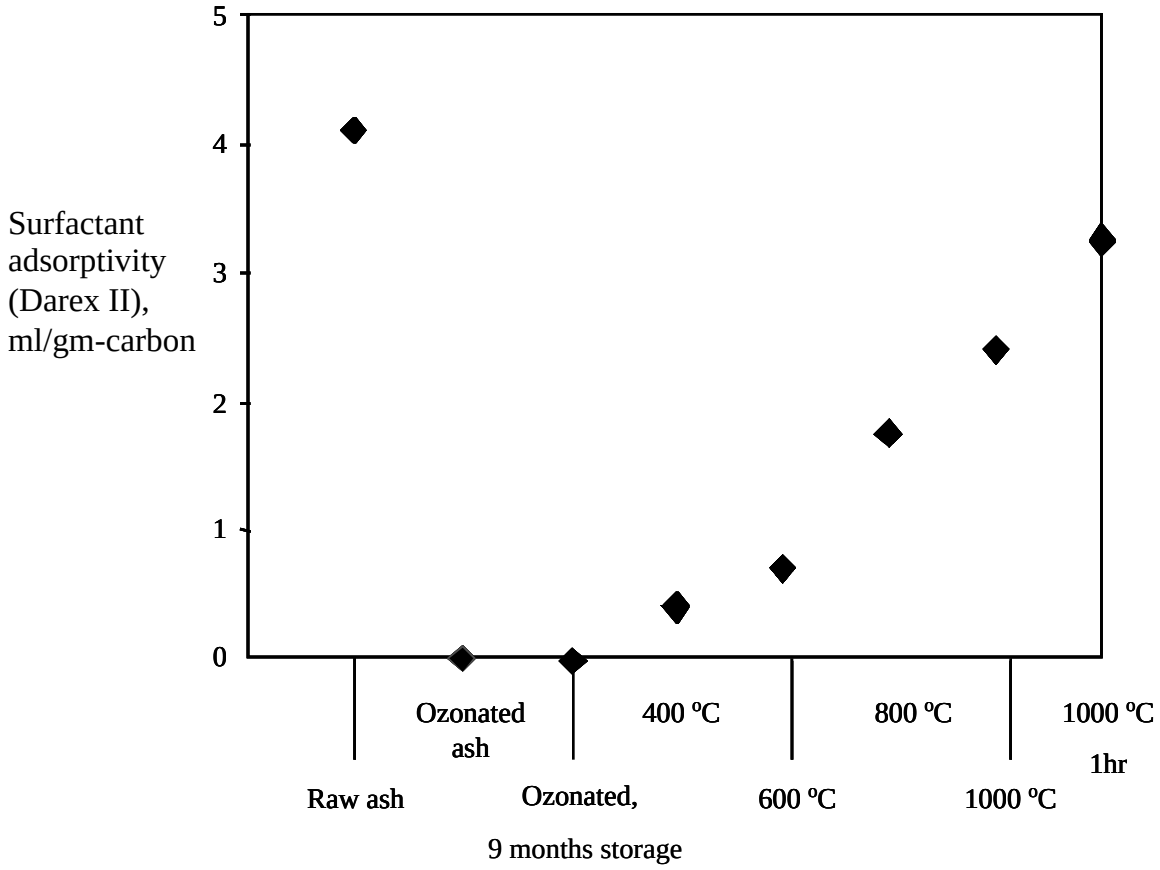

Figure 2.1 Effect of O_3 treatment on the adsorptivity of carbon-containing fly ash (Ash #1) toward the commercial anionic concrete surfactant, Darex II. The fly ash sample contains 6.3% carbon and derives from full-scale combustion of a bituminous coal. O_3 treatment at 20 °C: 20 gm-ozone/kg-ash. The figure shows the stability of the complexes at room temperature — 9 months of laboratory storage produced no measurable recovery of the adsorptivity. Data labeled 400-1000 °C represent ozonated samples subsequently treated in a preheated tube furnace in N_2 at the given peak temperature for 30 min except where marked.

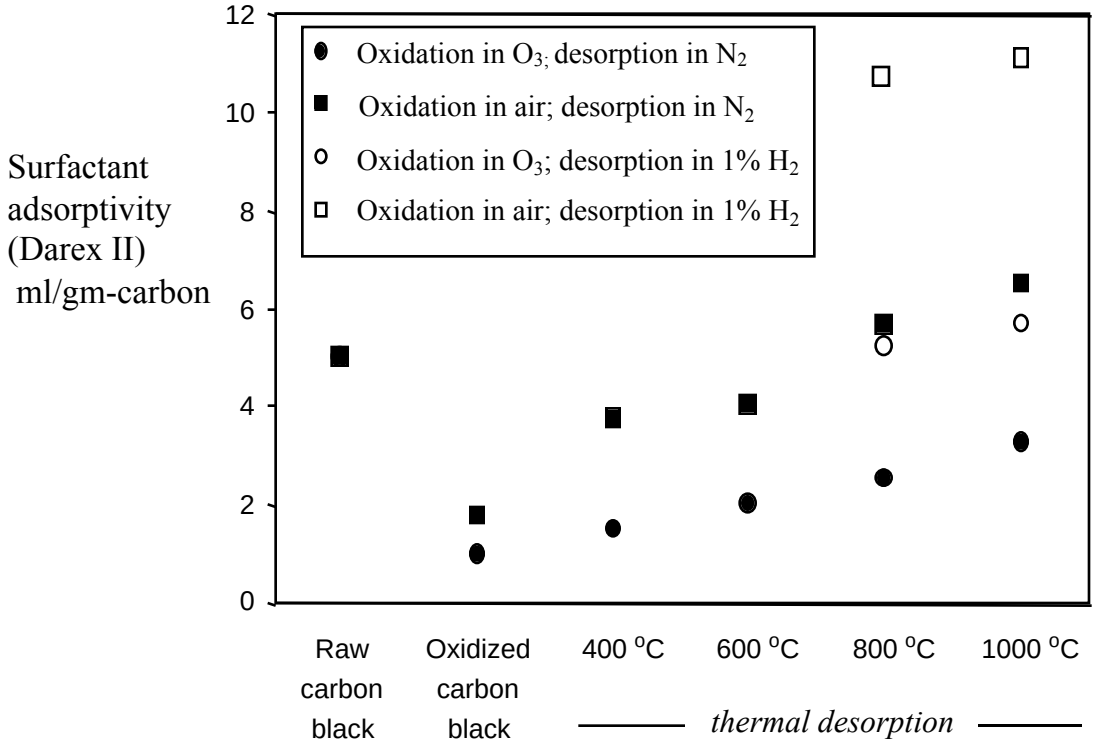

Figure 2.2 Effect of oxidation and subsequent thermal desorption on the surfactant adsorptivity of M120 carbon black. Air oxidation at 450 °C for 10 hrs (20% weight loss). O_3 treatment at 20 °C; 600 gm-O_3/kg-carbon. Data labeled 400-1000 °C represent ozonated samples subsequently treated for 30 min in a preheated furnace in N_2 or 1%v/v H_2/He at the given peak temperature.

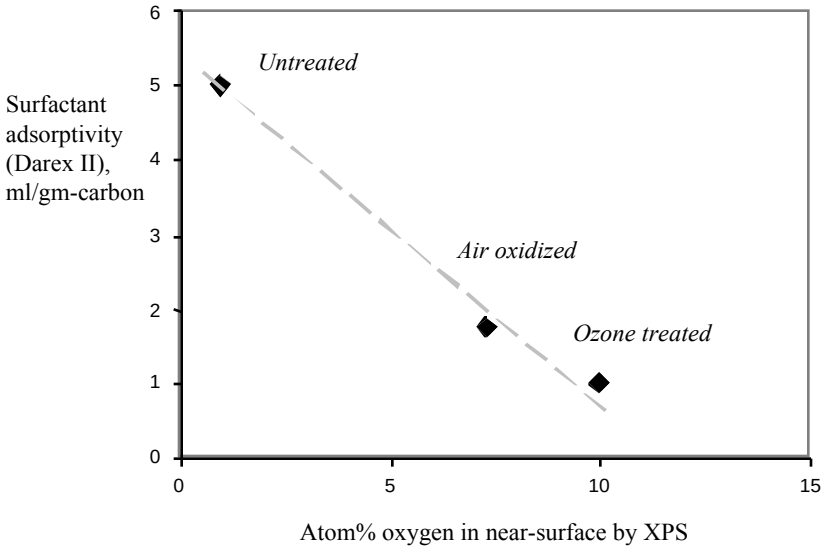

Figure 2.3 Near-surface atomic oxygen concentration by XPS and its inverse correlation with surfactant adsorptivity for M120 carbon blacks.

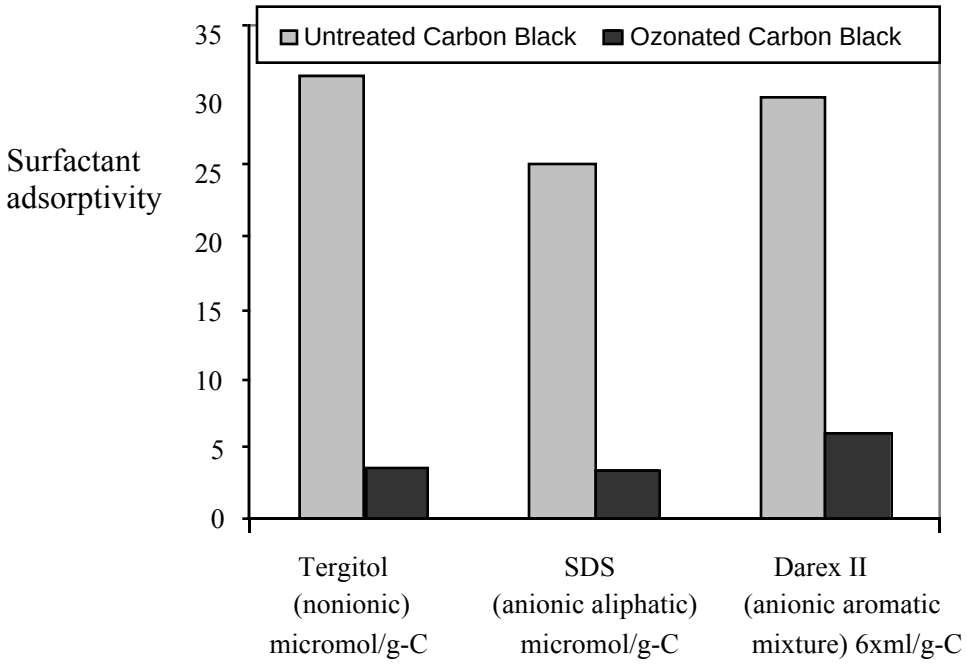

Figure 2.4 Effect of ozonation on the standard adsorptivity toward three surfactants of differing type. For the natural surfactant mixture, Darex II, the adsorbed amounts are presented as titrated solution volumes (6x ml surfactant solution/gm-carbon). Because of the need for different units, the absolute values in this figure are not meaningful, but rather the relative effect of ozonation for the three surfactants.

Table 2.2
Effect of ozonation on total carbon surface areas

Sample	*Surfactant Adsorptivity (ml / gm-carbon)*	*Carbon Surface Area (N_2 BET) (m^2 / gm-carbon)*
Ash #1 (FA21) from bitum. coal, 6.1% LOI	3.9	51.3
Ash #1 ozonated (2g O_3/kg ash)	0.8	38.1
Ash #1 heavily ozonated (20g O_3/kg ash)	0.0	26.3
Ash #2 (FA22) from bitum. coal, 33% LOI	2.8	50.4
Ash #2 ozonated (8g O_3/kg ash)	1.0	53.4

M120 Carbon black:		
Untreated	5	38.5
Air oxidized	1.75	234
Ozonated	1	36.7

Thermal desorption

Fig. 2.2 shows a rapid rise in adsorptivity with increasing thermal desorption temperature in the range of 600-1000 °C, consistent with previously observed peaks in TPD curves in that temperature range [21], which mark a region of significant surface oxide decomposition. Thermal desorption at 1000 °C in N_2 atmosphere reverses most of the effects of oxidation, but a modest hysteresis in surfactant adsorptivity was still observed. Using 1% H_2 atmosphere for thermal desorption makes the process fully reversible, suggesting that the hysteresis was due to the creation of new active sites during oxide decomposition which became chemisorptive sites for oxygen in room air during cooling or sample handling. H_2 treatment at high temperature is known to remove oxides, gasify the most reactive surface carbon atoms and to minimize O_2 re-adsorption at room temperature [30].

For air oxidized samples, thermal desorption at 1000 °C in N_2 raises the surfactant adsorptivity to values 30% above the pre-oxidation level, an effect which is likely related to the very significant surface area development accompanying air oxidation under our conditions. Finally, after treatment with 1% H_2 at 1000 °C, the surfactant adsorptivity of air oxidized carbon black is 225% of its initial value, which is not surprising, considering the effects of both the oxygen-free surface and the enhanced total surface area developed during air oxidation.

The large-sample thermal desorption experiment provides a useful count of the surface oxides (Fig. 2.5). Following either light ozonation (50 g-ozone/kg-carbon) or heavy ozonation (200 g-ozone/kg-carbon) the oxide count is 0.45-0.84 millimole oxide/g-carbon, which is comparable to the theoretical surface site density of 0.63 millimole/g estimated from the total surface area. It is noteworthy that ozone can quantitatively cover most of carbon black surfaces with oxides while there is insignificant carbon consumption by gasification. This behavior is in contrast to oxygen chemisorption, which typically covers only a fraction of the total surface when the chemisorption is carried out below gasification temperatures [31]. The quantitative surface coverage suggests that ozone can attack or reside not only on edges and defect sites but also on graphene basal sites. Such non-selective chemisorption has previously been observed for atomic oxygen [32]. Previous studies with ozone, however, have shown much smaller fractional surface coverage on graphite [21], a difference that may reflect the very different degrees of structural perfection in graphite and carbon black.

XPS analysis

Near-surface oxygen concentrations by XPS are much less than 100%, varying from 1% for the untreated carbon black to a maximum of 10% for the ozonated carbon black. The apparent discrepancy between XPS and thermal desorption reflects the sampling depth (electron escape depth) of the XPS technique which is about 8 nm under these experimental conditions and thus captures as many as 8 nm / 0.34 nm (single carbon atom layer thickness) ~ 23 subsurface carbon layers in addition to the oxygen-rich surface.

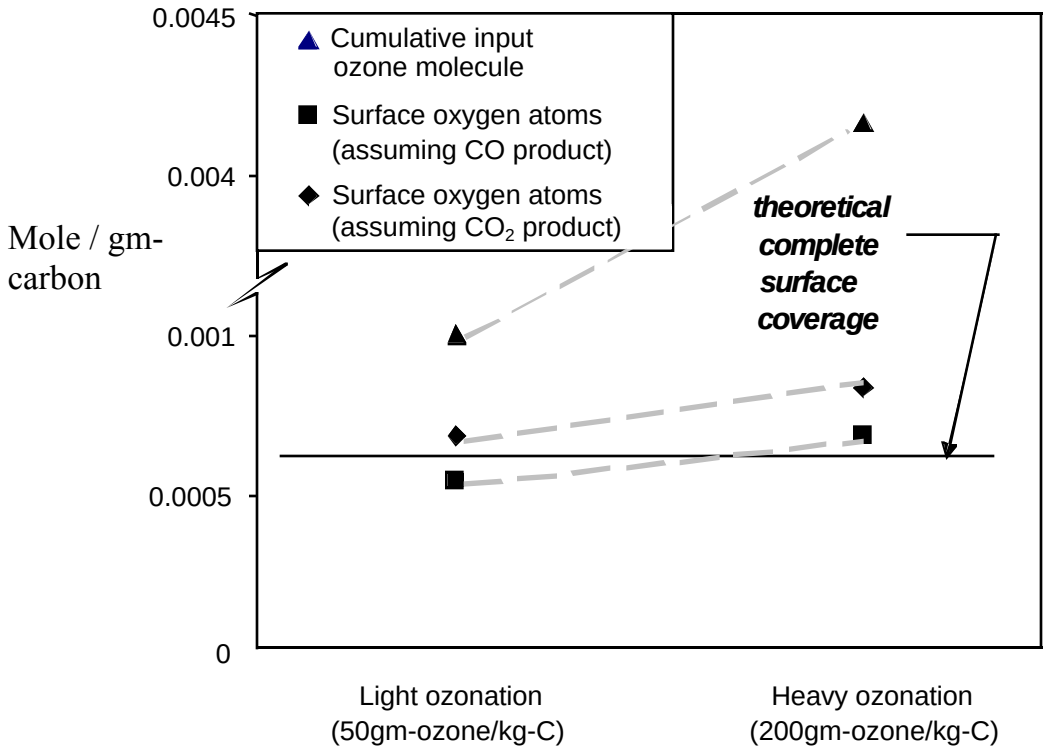

Figure 2.5 Oxide counts by thermal desorption. Weight loss determined by heating 150 mg sample in ultra high purity N_2 at 50 °C /min to 850 °C with a hold time of 30 min. Weight losses are 0.34% (untreated carbon black), 1.50% (light ozonation) and 1.85% (heavy ozonation). Plotted are the moles of surface oxygen atoms calculated from the above weight loss values assuming either CO or CO_2 product as bracketing cases. The total site number is estimated from N_2 BET area (38 m^2/g) assuming 10 A^2 per surface oxygen atom [41]. Ozone quantitatively covers the total surface with oxides. Also plotted for comparison are the total moles of O_3 introduced in the feed gas giving a measure of O_3 conversion efficiency to oxides.

The high-resolution C1s peak at around 285 eV shown in Fig. 2.6 exhibits a long tail on the high energy side similar to that reported by Wu et al [3]. Spectral analysis suggests a variety of band modes on the oxidized surfaces including C-O, C=O, and O-C=O. A clear feature in the C1s tail is the rise of a peak at around 289 eV during oxidation (by either air or ozone), a peak normally associated with O-C=O (carboxyl, anhydride or lactone). The lack of other distinct features makes the full quantitative spectral analysis uncertain, but it does suggest a higher concentration of C-O containing groups (e.g. phenol) in the air oxidized sample and a higher concentration of O-C=O groups in the ozone sample. Additional information is provided by the high resolution O1s peak, whose spectral analysis is shown in Table 2.3. The fraction of O-C is slightly higher for both the air oxidized and ozone treated samples than O=C.

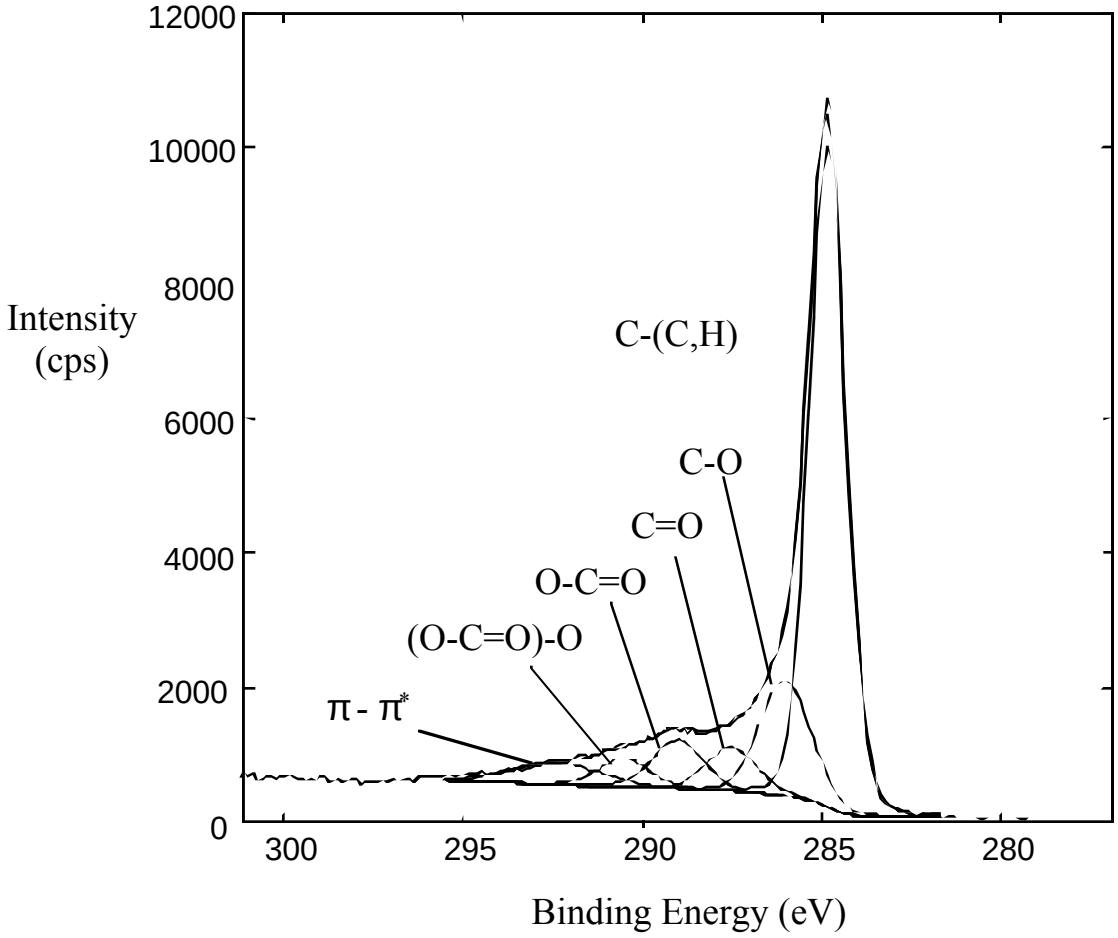

Figure 2.6 High resolution C1s XPS spectra of O_3 treated carbon black

Table 2.3
Area of O1s peak and near surface oxygen concentration of carbon blacks

	Normalized area of the O1s peaks (%)			
Carbon black	O-C	O=C	Others[1]	Oxygen (atom%)
Untreated	66	28	6	1
Air oxidized	50	38	13	7.3
O_3 treated	50	40	10	10

[1] Chemisorbed O_2/H_2O

FT-IR spectra analysis

Table 2.4 shows selected results of FT-IR characterization. A gross classification would associate the bands from 1600-1800 cm^{-1} primarily with carboxyl/carbonyl structures (C=O), and those from 1100-1400 cm^{-1} with phenolic or etheric structures (C-O) [33-35]. This is in agreement with the features seen in the XPS O1s peak and with some earlier studies of ozone treatment on carbon fibers [17]. Within the bands are specific peaks whose spectral locations vary between the air oxidized and ozonated carbon black samples. Table 2.4 gives possible assignments.

Table 2.4
Possible FT-IR peak assignments [30-32]

Wave number, cm^{-1}	Possible Peak Assignments
Air oxidized sample	
2340	CO_2 Contamination
1745	carboxylic acid – carbonyl stretch (C=O)
1600	carboxylate (COO-) –COO- stretch OR aromatic ring vibrations
1260	phenol –C-O stretch and O-H bend
O_3 treated sample	
2340	CO_2 Contamination
1890	lactone or anhydride or phenyl
1725	carboxylic acid C=O stretch
1690	aryl ketone C=O stretch
1640	aromatic ketone
1405	phenol COH bend or carboxylic acid

Previously published FT-IR spectra of oxidized carbons surfaces share many of the peaks identified in Table 2.4 [36, 37-41]. A notable difference is a peak around 1220 cm^{-1} in the ozonation studies of Smith [37,39], Sutherland [41] and Mawhinney [42] but absent here. Also, the peak around 1890 cm^{-1} that was observed here was not detected in previous studies. Previous authors assigned the peak around 1220 cm^{-1} to ester, lactone, aromatic ketone, or cyclic anhydride – consequences of a C-O stretch and an O-H bend. The differences between the spectra observed here and previous spectra may relate to reaction conditions (temperature, time) or to water/humid air exposure during handling. The peak around 1890 cm^{-1} was assigned to lactone or anhydride, suggesting these groups may be more prevalent during ozone treatment than during air oxidation. Indeed ozone can break unsaturated C=C bonds to yield unstable ozonides as intermediates, which may rearrange to produce anhydrides or lactones [40,42,43]. The presence of the 1260 cm^{-1} in the air oxidized but not the ozone treated sample suggests formation of more phenolic groups.

Although the oxygen bonding modes have been characterized by XPS and FT-IR, it should be mentioned that there is no evidence shows that the bonding mode is a deciding variable in the

suppression of surfactant adsorption. Although ozone is somewhat more effective than oxygen under the conditions used, the degree of adsorption suppression correlates adequately with the different *amounts* of surface oxides, as also seen by Wu et al. [3] for the anionic surfactant dodecanoic acid on carbon.

Hygroscopic and acidic properties

DSC traces were obtained for untreated and oxidized carbon black samples. No large heat effects are seen relative to untreated carbon black except for the temperature at 100-180 ^{o}C, which is just visible for the ozonated sample and quite pronounced for the air oxidized sample. Repeated experiments on a single air oxidized sample show this peak only on the first scan, so it represents an irreversible process. The temperature range suggests water desorption, so a special test was devised to characterize the hygroscopic nature of the oxidized samples.

Fig. 2.7 shows that both methods of oxidation make the carbon black samples quite hygroscopic. The large difference between 12 hour and 7 day exposure in almost saturated humidity for ozone treated sample may reflect a slow hydration of anhydride sites. Heating at 1000 ^{o}C removes the hygroscopic behavior for the ozonated sample as expected, but surprisingly the air-oxidized sample retains much of its hygroscopic behavior after thermal desorption. The surface areas of the air oxidized samples are 234-246 m^2/g — a factor of about 7 times higher than the ozonated samples (34-40 m^2/gm) and it is likely that the high water uptake in the air oxidized/thermally desorbed sample is due to adsorption and capillary condensation in fine porosity developed during air oxidation. Integration of the DSC difference curve of air oxidized sample gives an amount of heat that is somewhat greater than but of the same order of magnitude as the vaporization of bulk water at about 20% of the sample mass. Overall, thermal desorption of adsorbed/condensed water in fine porosity is thus the most likely explanation for the main origin of the irreversible endotherm at 130 ^{o}C seen in the DSC of air oxidized samples and, to a much less extent, for the ozonated samples. The absence of other peaks indicates that no significant endothermic/exothermic rearrangement or desorption occurs. This result suggests that any removal of unstable ozonides or peroxides must have occurred during reaction or sample handling (prior to DSC) and that much of the oxide desorption does not occur under 600 ^{o}C, the maximum DSC temperature.

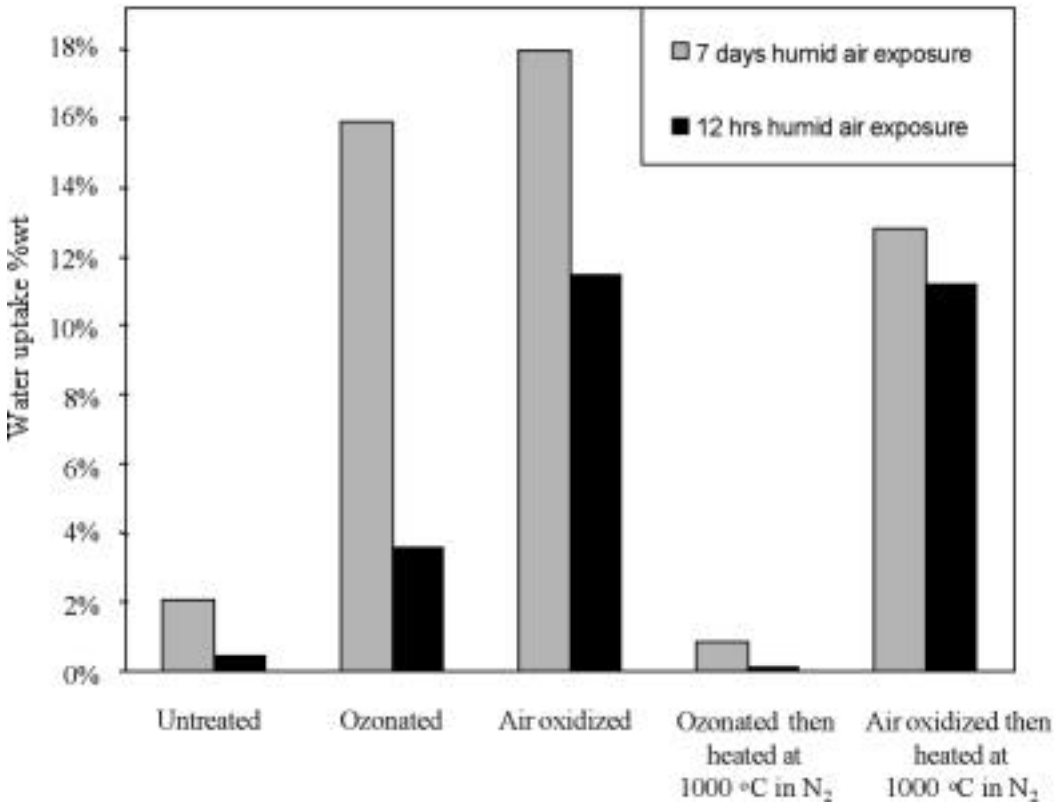

Figure 2.7 Effect of surface oxidation and subsequent thermal desorption on hygroscopic behavior of carbon black samples.

Fig. 2.8 shows the pH of raw and treated carbon black slurries. Both oxidation methods introduce primarily acidic oxygen complexes, which is consistent with the carboxylic functionalities seen by FT-IR. It is notable that the ozonated sample after thermal desorption not only loses its acidity but exhibits a pH of 9.2. This significant basicity is due either to residual refractory basic oxides, or more likely to the higher concentration of oxygen-free Lewis base sites associated with π cloud systems [15, 44].

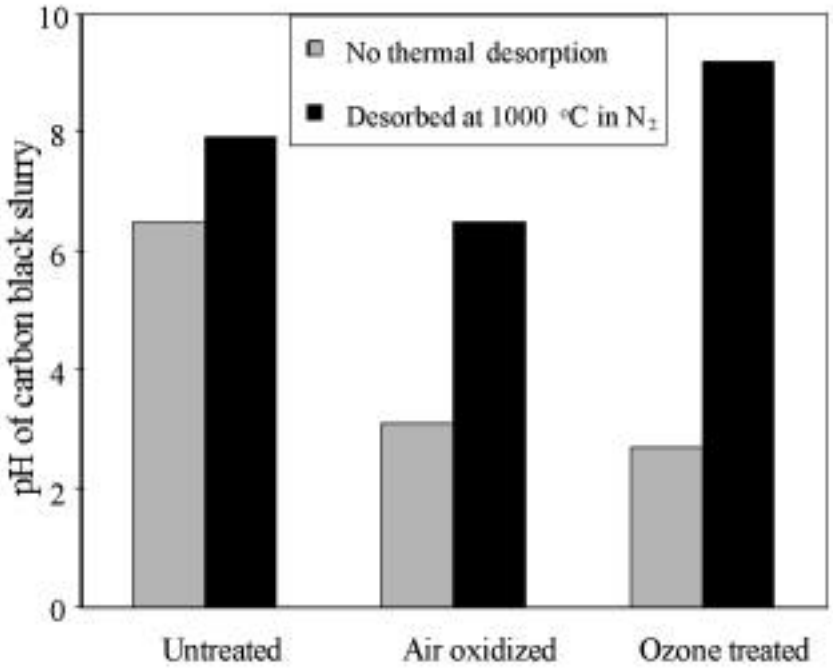

Fig. 2.8 The pH of raw, oxidized, and thermally desorbed carbon blacks by ASTM 1512-95.

Carbon surface energy analysis

Table 2.1 shows that both modes of surface oxidation improve the wetting (reduce the contact angle) of the two standard liquids: benzyl alcohol and nitromethane. Because benzyl alcohol and nitromethane have different fractional polarities (22% vs. 40%), they can be used to derive the polar and dispersive components on solid surface tension.

The determination of carbon surface energies by the Fowkes / Owens-Wendt theory [45] will prove useful for elucidating the mechanism of oxidative adsorption suppression. This theory of interfacial interaction divides the total solid surface energy into polar and dispersive components:

$$\gamma_s = \gamma_s^p + \gamma_s^d \qquad (2.1)$$

The liquid surface tension is likewise divided into polar and dispersive components:

$$\gamma_l = \gamma_l^p + \gamma_l^d \qquad (2.2)$$

The liquid/solid interfacial energy is expressed as:

$$\gamma_{sl} = \gamma_s + \gamma_l - 2(\gamma_s^d \gamma_l^d)^{1/2} - 2(\gamma_s^p \gamma_l^p)^{1/2} \qquad (2.3)$$

Combining these relations with the Young equation:

$$\gamma_s = \gamma_{sl} + \gamma_l \cos\theta \qquad (2.4)$$

yields:

$$(\cos\theta + 1)\gamma_l = 2(\gamma_s^d \gamma_l^d)^{1/2} + 2(\gamma_s^p \gamma_l^p)^{1/2} \qquad (2.5)$$

If contact angle, θ, is measured for a test liquid of known γ_l^d and γ_l^p, only two unknowns remain in Eq. 5: γ_s^d and γ_s^p. Measuring θ for a second test liquid provides the second equation needed to calculate γ_s^d and γ_s^p and their sum, the total solid surface energy, γ_s.

The result of this calculation for our carbon surface is shown in Table 2.5. Both air and ozone oxidation greatly enhances the polar contribution to carbon black surface energy, with ozone treatment showing the larger effect. The dispersive component of surface energy is observed to increase as well, though only modestly, so the net effect of oxidation is a rather large increase in total surface energy (polar plus dispersive). An increase surface energy normally brings about an increase in the strength of interfacial forces, which thus promotes wetting (as observed) and promotes adsorption from the vapor phase. The opposite behavior in solution (adsorption suppression) has been attributed to the fact that adsorption from solution is governed not only by surface/adsorbate forces, but also by surface/solvent interactions and solvent/adsorbate interactions. This idea is discussed in detail below.

Table 2.5
Carbon black surface energies
and their dispersive and polar components[1]

	γ_s^d (mJ/m^2)	γ_s^p (mJ/m^2)	γ_s (mJ/m^2)
Untreated	20.9	0.9	21.8
Air oxidized at 450 °C, 10 hrs	22.7	4.3	27.0
Treated in 2 wt-% O_3 (600 g- O_3/kg-C)	24.4	8.1	32.5

[1]Determined by Owens-Wendt theory using benzyl alcohol and nitromethane as standard reference liquids

Mechanisms of Adsorption Suppression

Carbon surface oxidation can either promote or inhibit adsorption of organics from aqueous solution depending on the nature of oxide, adsorbate, and the solution chemistry. Adsorption can be influenced by surface charge, van der waals forces, hydrogen bonding, $\pi-\pi$bonding (for aromatic surfactants on carbon), hydrophobic interactions, chemisorption and electron transfer complexes[14]. In principle the same factors are relevant for surfactant adsorption, along with additional factors such as adsorption of hemi-micelles and dual site adsorption involving adjacent polar and nonpolar surface functionalities. However, in the search for mechanism, the experimental result shows that oxidation suppresses adsorption with almost equal effectiveness for a variety of carbon types, oxidants, and surfactant types. It suggests a simple mechanism common to all surfactant/carbon systems studied here. Based on other aqueous phase adsorption systems, several

possible mechanisms have been considered about the surfactant adsorption suppression by surface oxidation:

1. Micropore blockage. Surface oxide formation decreases total area by blocking fine pores or pore mouths.

2. Electron withdrawal. The addition of electronegative oxygen atoms to graphene layer edges withdraws electron density from the π clouds and reduces dispersion forces that bind the adsorbate to graphene basal surface [14].

3. Electrostatic repulsion. The acidic nature of most carbon surface oxides leads to a negatively charged surface in the high-pH concrete solution. The net negative surface charge repels anionic (negatively charged) surfactant molecules [14].

4. Reduction of hydrophobic interactions. Introduction of oxides destroys nonpolar surface area that is responsible for adsorption, leaving hydrophilic surface sites that participate in strong hydrogen bonding with water and are effectively unavailable for surfactant adsorption.

5. Steric hindrance. Introducing surface functionality disrupts the close geometric accommodation between the adsorbate and the surface thus reducing the overall strength of attractive forces. This effect would be most important for large adsorbates and those capable of $\pi-\pi$bonding which relies on the atomic flatness of graphene basal plane segments.

The present data allows a critical evaluation of these completing explanations for our system as follows. Mechanism 1 (pore blockage) is a contributor for at least some fly ash carbons, but is not believed to the primary mechanism, since carbon black and some other fly ash carbons exhibit the same beneficial effect of ozonation, but do not show any decrease in area.

Mechanism 2 (electron withdrawal) can be ruled out by the surface energy results derived from wetting studies (Table 2.5). Ozonation is seen to add a polar component to the surface energy without decreasing the dispersive component. Indeed the dispersive component *increases* slightly and the overall effect is a large increase in total surface energy. Thus ozonation is expected to slightly *enhance* the dispersive attractive forces for adsorption, not *suppress* them.

Mechanism 3 (electrostatic repulsion) likely plays a role for resin-derived concrete surfactants, since they are anionic and would be repelled by the negative surface charges expected on the oxidized carbon surfaces at the high pH of concrete paste. This mechanism is not believed as the primary effect, since surface oxidation by ozone is also effective at suppressing the adsorption of Tergitol, a nonionic surfactant.

Mechanism 4 (reduction of hydrophobic interactions) is believed to the primary mechanism sufficiently to explain the main effects observed in this study. It can be arrived by basic consideration of the nature of surfactants. Any solution adsorption process can be broken down into three conceptual steps: 1. desolvation of solute, 2. desolvation of surface, and 3. solute/surface interaction. The total driving force for adsorption is the sum of the driving forces (chemical potential differences) of the three steps. Unlike other solutes, surfactants have a highly insoluble

nonpolar part, for which step 1 (desolvation) is highly favorable, and thus the driving force for step 1 can be sufficient to drive adsorption. This fact is evident from the propensity that surfactant molecules collect at the gas interface, chiefly in bubble cavities, which offer no attractive interfacial forces (no driving force component for step 3). Nonpolar solid surfaces behave in similar fashion. Step 1 and 2 are the “hydrophobic forces” that drive surfactants to nonpolar surfaces, and when these "forces" are strong the adsorption is not dependent on the driving force for step 3 or on the detailed nature of the surface, as long as it is nonpolar. It is believed that the surfactant adsorptivity of carbon is most directly related to the fraction of its surface that is hydrophobic (nonpolar) with other characteristics of the surface being of secondary importance, as also cited by Wu[3]. Ozonation destroys this nonpolar surface and replaces it with oxidic surface that is hydrophilic and capable of strong hydrogen bonding with the solvent water. Since adsorption in aqueous solution is intrinsically a competitive process in which the surfactant and water molecules compete for adsorption sites, the water molecules have a strong advantage over the surfactant molecules on oxide-covered surfaces and the overall effect is suppression of the surfactant adsorptivity.

Mechanism 5 (steric hindrance), or geometric mismatch between sorbent/surface, is not believed to be the primary mechanism here. Oxidation most certainly changes the atomic topology of the carbon surface, but the wetting studies show enhanced dispersion interactions with both benzyl alcohol and nitromethane. The surfactant molecules being larger are more prone to steric effects, but the two chain surfactants should have flexibility to adapt to irregular surfaces. This mechanism is expected to be most important for aromatic or polyaromatic solutes that adsorb on carbon through $\pi-\pi$bonding, which is not the case for the surfactants investigated here. Although steric effects are not the primary mechanism, it is believed that they play a role in determining the amount of surface oxides needed for the hydrophobic mechanism (mechanism 4) to engage. As oxide coverage increases, it becomes increasingly difficult for the large nonpolar segments of the surfactant to find a nonpolar surface patch lying between oxide sites. Further, oxides serve as nucleation sites for hydrogen-bonded clusters of water molecules, thus enlarging their effective size for the disruption of the continuous nonpolar surface. Through this mechanism significant adsorption suppression is expected at coverage much less than 100%, as observed in our previous study [7].

The results in this report help explain the origin of apparently contradictory reports of the effects of surface oxidation in the literature on fly ash carbon [8,9,12]. It is believed that the enhanced uptake of polar compounds from the vapor phase (acetone) [9] is driven by the increased surface energy and polarity of oxidized carbon surfaces, while the decreased uptake of surfactant from solution is related not to the magnitudes of the energies but to the increased polar/dispersive ratio. Vapor phase adsorption is driven only by step 3 — surface/vapor attractive forces, which are increased by oxidation and adsorption (like wetting) is enhanced. In solution the overall surface energy is less important than the polar/dispersive ratio since adsorption is competitive and the polar/dispersive ratio governs the relative affinity for water and surfactant molecules. More detailed surface characterization would yield further insight into the nature of the specific oxygen functionalities, but may not contribute significantly to the understanding of surfactant adsorption.

Because the proposed mechanism is based on hydrophobic interactions, which are the essence of surfactant action, it offers a convenient explanation for the general nature of the phenomenon observed — the fact that surface oxidation is effective over a range of carbon/surfactant/oxidant types. Surface oxygen complexes may still interact with the polar or ionic groups in surfactants [3,

46], but the dominance of hydrophobic interactions makes these specific interactions of secondary importance in the present system, and indeed their effects are difficult to discern in the data.

Conclusions

A battery of carbon surface analyses has been used to study the underlying mechanisms behind the previously reported ozone treatment effect on surfactant adsorption [7]. Ozone increases surface energy but suppresses adsorption in each carbon/surfactant system studied. Air oxidation produces a similar effect although it produces somewhat different surface species, notable more phenol and less lactone/anhydride. The overall extent of adsorption suppression correlates with surface oxygen concentration by XPS and is largely, though incompletely, reversible upon thermal desorption in N_2. The effects of surface oxidation are quite similar for three surfactant types: a nonionic, an aliphatic chain anionic, and a globular anionic mixture derived from natural sources. The combined data indicate that the primary mechanism of adsorption suppression is the destruction of nonpolar carbon surface area with possible contributions from blockage and increased negative surface charge for some systems.. While the polar/ionic portion of surfactants can undergo specific interactions with surface oxygen complexes, here these effects are secondary compared to the amount of nonpolar surface on which surfactant adsorption is strongly favored by hydrophobic interactions.

References for Chapter 2

1. Pavan PC, Crepaldi EL, Gomes GA, Valim JB. Adsorption of sodium dodecylsulfate on a hydrotalcite-like compound. Effect of temperature, pH and ionic strength. Colloid Surf A. 1999;154(3):399-410.
2. Brown W, Zhao J. Adsorption of sodium dodecyl sulfate on polystyrene latex particles using dynamic light scattering and zeta potential measurements. Macromolecules 1993; 26(11):2711-2715.
3. Wu SH, Pendleton P. Adsorption of anionic surfactant by activated carbon: effect of surface chemistry, ionic strength, and hydrophobicity. J Colloid and Interface Sci 2001; 243(2):306-315.
4. Garcia-Delgado RA, Cotoruelo LM, Rodriguez JJ. Adsorption of anionic surfactant mixtures by polymeric resins. Sep Sci Technol 1992; 27(8-9):1065-1076.
5. Freeman E, Gao YM, Hurt RH, Suuberg EM. Interactions of carbon-containing fly ash with commercial air-entraining admixtures for concrete. Fuel 1997; 76(8):761-765.
6. Gao Y, Shim H, Hurt RH, Suuberg EM, Yang NYC. Effects of carbon on air entrainment in fly ash concrete: The role of soot and carbon black. Energy Fuels 1997; 11(2):457-462.
7. Gao Y, Kulaots I., Chen X, Aggarwal R, Mehta A, Suuberg EM, Hurt RH. Ozonation for the chemical modification of carbon surfaces in fly ash. Fuel 2001; 80(5):765-768.
8. Hill RL, Sarkar SL, Rathbone RF, Hower JC. An examination of fly ash carbon and its interactions with air entraining agent. Cem Concr Res 1997; 27(2):193-204.
9. Hill R, Rathbone R, Hower JC, Investigation of fly ash carbon by thermal analysis and optical microscopy. Cem Concr Res 1998; 28(10):1479-1488.
10. Helmuth RA. Fly ash in cement and concrete. Skokie, Illinois: The Portland Cement Association, 1987:79-82
11. Yu J, Külaots I, Sabanegh N, Gao Y, Hurt RH, Suuberg, EM, Mehta A. Adsorptive and optical properties of fly ash from coal and petroleum coke co-firing. Energy Fuels 2000; 14(3):591-596.
12. Hachmann L, Burnett A, Gao YM, Hurt RH, Suuberg EM. Surfactant adsorptivity of solid products from pulverized coal combustion under controlled conditions. Proceedings of the Combustion Institute. 1998; 27:2965-2971.

13. Beck NV, Meech SE, Norman PR, Pears LA. Characterization of surface oxides on carbon and their influence on dynamic adsorption. Carbon 2002; 40(4):531-540.
14. Radovic LR, Moreno-Castilla C, Rivera-Utrilla J. Carbon materials as adsorbents in aqueous solutions. In Radovic LR editor. Chemistry and Physics of Carbon, Vol. 27. New York: Marcel Dekker, 2001:227-382.
15. Lopez-Ramon MV, Stoeckli F, Moreno-Castilla C, Carrasco-Marin F. Specific and non-specific interactions of water molecules with carbon surfaces from immersion calorimetry. Carbon 2000; 38(6):825-829.
16. Domingo-Garcia M, Lopez-Garzon FJ, Perez-Mendoza M. Effect of some oxidation treatments on the textural characteristics and surface chemical nature of an activated carbon. J Colloid Interface Sci 2000; 222(2):233-240.
17. Fu X, Lu W, Chung DDL. Ozone treatment of carbon fiber for reinforcing cement Carbon 1998; 36(9):1337-1345.
18. Gomez-Serrano V, Alvarez PM, Jaramillo J, Betran FJ. Formation of oxygen complexes by ozonation of carbonaceous materials prepared from cherry stones I. Thermal effects. Carbon 2002; 40(4):513-522.
19. Gomez-Serrano V, Alvarez PM, Jaramillo J, Betran FJ. Formation of oxygen complexes by ozonation of carbonaceous materials prepared from cherry stones II. Kinetic study. Carbon 2002; 40(4):523-529.
20. Kotzick R, Panne U, Niessner R. Changes in condensation properties of ultrafine carbon particles subjected to oxidation by ozone. J Aerosol Sci 1997; 28(5):725-735.
21. Magne P, Dupont-Pavlosky N. Graphite-ozone surface complexes. Carbon 1988; 26(2):249-255.
22. Rakitskaya TL, Bandurko AY, Ennan AA, Litvinskaya VV. Kinetics of the low- temperature decomposition of ozone by carbon fiber materials. Kinet Catal 1994; 35(5):763-765.
23. Stephens S, Rossi MJ, Golden DM. The heterogeneous reaction of ozone on carbonaceous surfaces. Int J Chem Kinet 1986; 18:1133-1149.
24. Takeuchi Y, Itoh T. Removal of ozone from air by activated carbon treatment. Sep Technol 1993; 3(3):168-175.
25. Papirer E, Donnet J-B, Schutz A. Etude cietique de l'oxydation des noirs de carbone par l'ozone. Carbon 1967; 5:113-125.
26. Mul G, Neeft JPA, Kapteijn F, Moulijn JA. The formation of carbon surface oxygen complexes by oxygen and ozone. The effect of transition metal oxides. Carbon 1998; 36(9):1269-1276.
27. Washburn EW. The dynamics of capillary flow. Phys Rev 1921; 17(3):273-283.
28. Dietz VR, Bitner JL. The reaction of ozone with adsorbent charcoal. Carbon 1972; 10:145-154.
29. Dietz VR, Bitner JL. Interaction of ozone with adsorbent charcoals. Carbon 1973; 11:393-401.
30. Menendez JA, Phillips J, Xia B, Radovic LR. On the modification and characterization of chemical surface properties of activated carbon: In the search of carbons with stable basic properties. Langmuir 1996; 12(18):4404-4410.
31. Haynes, BS. A turnover model for carbon reactivity I. Development. Combust Flame 2001; 126(1-2): 1421-1432.
32. Leon CA, Leon Y, Solar JM, Calemma V, Radovic LR. Evidence for the protonation of basal plane sites on carbon. Carbon 1992; 30(5):797-811.
33. Dyer JR. Applications of absorption spectroscopy of organic compounds. Englewood Cliffs NJ: Prentice Hall. 1965:33-38.
34. Lambert JB, Shurvell HF, Verbit L, Cooks RG, Stout GH. Organic structural analysis. New York: Macmillan Publishing Co., 1976:234-241.
35. Biniak, S, Szymanski G, Siedlewski J, Swiatkowski A. The characterization of activated carbons with oxygen and nitrogen surface groups. Carbon 1997; 35(12):1799-1810.
36. Tognotti L, Petarca L, D'Alessio A, Benedetti E. Low temperature air oxidation of coal and its pyridine extraction products. Fuel 1991; 70(9):1059-1064.
37. Smith DM, Chughtai AR. The surface structure and reactivity of black carbon. Colloid Surf A 1995; 105(1):47-77.

38. Akhter MS, Chughtai AR, Smith DM. Spectroscopic studies of oxidized soots. Appl Spectrosc 1991; 45(4):653-665.
39. Smith DM, Welch WF, Jassim JA, Chughtai AR, Stedman DH. Soot-ozone reaction kinetics: Spectroscopic and gravimetric studies. Appl Spectrosc 1988; 42(8):1473-1482.
40. Chughtai AR, Jassim JA, Peterson JH, Stedman DH, Smith DM. Spectroscopic and solubility characteristics of oxidized soots. Aerosol Sci Technol 1991; 15(2):112-126.
41. Sutherland I, Sheng E, Bradley RH, Freakley PK. Effects of ozone oxidation on carbon black surfaces. J Material Sci 1996; 31(21):5651-5655.
42. Mawhinney DB, Yates JT. FT-IR study of the oxidation of amorphous carbon by ozone at 300K-direct COOH formation. Carbon 2001; 39(8):1167-1173.
43. Criegee R. Mechanism of ozonolysis. Angewandte Chemie International Edition. 1975; 14(11):745-752.
44. Marsh H, O"Hair TE, Wynne-Jones Lord, The Carbon-Atomic Oxygen Reaction—Surface-Oxide formation on paracrystalline carbon and graphite. Carbon 1969; 7:555-566.
45. Owens DK, Wendt RC. Estimation of the surface free energy of polymers. J of Appl Polym Sci 1969; 13:1741-1747.
46. Zettlemoyer AC, Pendleton P, Micale FJ. Heats of immersion of microporous solids. In Ottewill RH, Rochester CH and Smith AL, editors. Adsorption from Solution. Bristol: Academic, 1983:113-127.

Chapter 3. Effect of Fuel Type and Combustion Conditions on Residual Carbon Properties and Fly Ash Quality

Background

Incomplete combustion of pulverized fuel can lead to significant decreases in thermal efficiency, operational problems with electrostatic precipitators, increased landfill volume for ash disposal, and loss of fly ash marketability. The high burnout efficiencies of most modern plants (> 99.5%) leave only modest room for improvement in efficiency, so much of the interest in residual carbon stems from problems with ash utilization in concrete. In fly ash concrete, carbon is an impurity that can discolor, increase water demand, and interfere with air entrainment. In some regions of the world the most serious problem with carbon is its undesirable effect on the air entrainment process. Carbon adsorbs the surfactants or "air entraining admixtures" used to stabilize air bubbles that impart freeze/thaw resistance in the set concrete[1-4].

Chronic problems with residual carbon in commercial ash samples have prompted a significant research effort over the last several years on various aspects of the problem, including techniques for predicting residual carbon levels[5-7], material properties of residual carbon[8], post-combustion processes for carbon/ash separation or low-temperature burnout[9], processes for carbon surface passivation to improve air entrainment behavior in fly ash concrete[10], and novel uses for high carbon ash or for concentrated residual carbon streams[11]. A series of recent studies on commercial ash samples has attempted to relate fly ash quality (surfactant adsorptivity) to residual carbon properties, such as surface area, surface chemistry, and pore size distribution[2-4]. This cited work does not provide direct answers to two important practical questions: how are adsorptivity and other residual carbon properties influenced by (1) solid fuel type, and (2) combustion conditions. These two questions lie in the realm of combustion science, a field that has not yet turned its attention to the issue of residual carbon *properties*. There are no measurements of residual carbon properties for a wide range of fuel types, nor for different temperature or oxygen histories experienced by a given fuel. Regarding firing conditions, a key unanswered question is the mechanism of unburned carbon formation in low-NO_x systems. Are the residual carbon problems widely observed after low-NO_x retrofits exclusively due to increased *amounts* of carbon in ash, or are chars formed in low-NO_x flames also highly adsorptive and thus intrinsically "bad"?

The present work address the effects of fuel and firing conditions on residual carbon properties by combining (1) laboratory-scale experiments on a range of fuels under common conditions, (2) pilot-scale experiments on a single burner facility operated in high and low-NO_x firing modes, and (3) the analysis of a large set of ash samples from full-scale commercial units.

Materials and Experimental Procedures

Table 3.1 gives properties of the solid fuels used in the bench- and pilot-scale experiments. In addition a set of 53 commercial ash samples were acquired from North American utility companies burning a range of bituminous and sub-bituminous coals[12]. One sample originated from a coal/petroleum-coke cofiring test burn described previously[3]. Selected measurements were also made on commercial carbon blacks (Cabot, Billerica, MA) as model materials for studying the effects of carbon surface oxides by X-ray Photoelectron Spectroscopy (XPS) in the absence of interference from the abundant inorganic oxides in ash.

Table 3.1
Properties of Laboratory and Pilot-Scale Fuel Samples

Sample	Ash	VM	C	H	O	N	S
	db wt-%	daf wt-%					
Laboratory fuels							
Tosco fluid petroleum coke	< 0.0005	6.17	87.38	2.41	5.14	2.57	2.5
Lei-Yang anthracite	22.34	7.27	90.47	2.01	5.86	0.717	0.93
Pocahontas #3 lv-bit. coal	4.6	19.19	89.87	4.9	1.14	0.78	3.31
Illinois #6 hv-bit. coal	16.16	45.49	78.11	5.44	9.73	1.32	5.39
Beulah lignite	9.56	62.01	73.14	4.46	20.59	1.00	0.82
Hard wood	0.52	80.64	45.58	6.17	47.81	0.151	0.03
Pilot-scale coals							
Huntington Utah hvB bit.	9.32	44.36	80.0	6.12	11.73	1.50	0.69
Illinois hvC bit.	12.71	42.7	76.26	5.38	12.46	1.51	4.38

Pilot-scale experiments in different high- and low-NO_x firing modes were carried out in a 29-kW, down-fired, U-shaped furnace with an inside diameter of 0.17 m and an overall length of 7.3 m. The furnace has a Reynolds number based on furnace diameter of 1000-2000 depending on stoichiometric ratio and temperature. The furnace was operated in unstaged, high-NO_x mode and in various low-NO_x modes with nominal 1.5 sec residence time in the fuel-rich zone. Temperatures 2 m from the burner ranged from 1720 - 1800 K and the furnace exit oxygen concentrations were 3-4%. The detailed furnace conditions are documented elsewhere[13]. The fly ash samples were collected by drawing the entire exit gas flow through a one-bag fabric filter.

In separate experiments partially combusted chars were generated from six pulverized solid fuels in a high-temperature entrained flow reactor by rapid-quench extractive sampling at residence times from 30 - 100 msec by a procedure described elsewhere[14]. The reactor is fed by a Hencken burner (Research Technologies, Pleasanton, CA) fueled with a CH_4 / O_2 / Ar mixture, producing a hot gas stream with post-flame oxygen concentration 13 mole-% oxygen (for the anthracite and coke) and 3 mol-% oxygen (for the wood and remaining coals). Centerline temperatures varied from 1300 K to 1650 K and the solids feed rate was limited to less than 1 gm/hr, yielding dilute phase conditions in which particle-to-particle interaction is minimal. Finally, selected char and ash samples were surface oxidized by contact with ozone-containing air passed upward through a fixed bed of material as in Gao et al.[10], or by subjecting samples to slow air oxidation in an open alumina crucible placed in a muffle furnace.

For each of the laboratory-, pilot-, full-scale, and surface oxidized samples, surfactant adsorptivity was measured by a modified foam index test, which is a standard titration procedure involving calibrated volumetric addition of surfactant solution to a cement / ash mixture as described in detail

elsewhere[2]. Char oxidation reactivities were measured by non-isothermal TGA using a heating rate of 30 K/sec in air. The relative reactivities are reported as values of critical temperatures, T_{cr}, defined as the temperature at which the measured rate reaches 0.065 mg/min-mg-partially-reacted-sample[15]. Under these conditions, the combustion rate is free from boundary layer or in-bed heat and mass transfer effects and thus represents a material property of the char sample. Nitrogen adsorption isotherms at 77 K were measured using an Autosorb vapor adsorption apparatus. Surface areas were computed using a 20 point BET algorithm and mesopore size distributions were computed from the Barrett, Joiner, and Hallenda (BJH) theory of simultaneous capillary condensation and multilayer adsorption[16]. The surface chemistry of raw, air oxidized, and ozonated carbon black samples was investigated by XPS carried out at Evans East Laboratories (East Windsor, New Jersey).

Results

Properties of the 53 commercial scale ash samples are summarized in Figs. 3.1 and 3.2. Residual carbon in class C ashes (primarily from sub-bituminous coals) tends to have a significantly higher combustion reactivity (low T_{cr} in Fig. 3.1) and higher surface areas (Fig. 3.2) than residual carbon in class F ashes (primarily from bituminous coals). Typical T_{cr} values are 450 ^{o}C (Class C) and 600 ^{o}C (Class F), which corresponds to a reactivity ratio of about 65 when the data is brought to a common reference temperature using an activation energy of 35 kcal/mol. This is a very significant reactivity difference and implies that in the secondary carbon burnout processes currently under

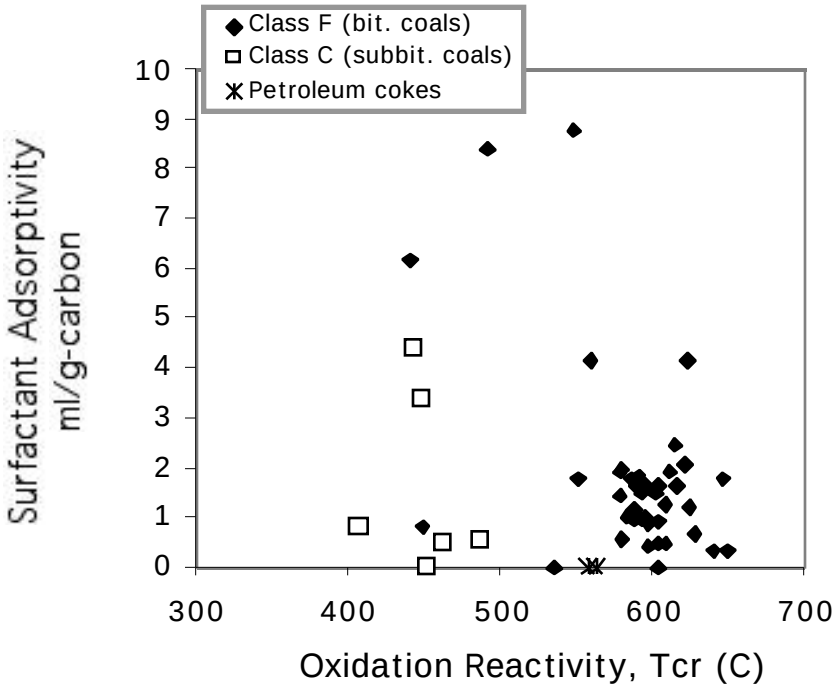

Figure 3.1 Combustion reactivities of residual carbon in 53 commercial pulverized fuel ash samples expressed as critical temperatures, T_{cr} values, derived from non-isothermal TGA experiments.

development, class C ashes can be beneficiated at significantly lower temperatures than class F ashes. The higher areas of sub-bituminous carbon residues also make them more attractive as

inexpensive environmental sorbents, but this advantage is diminished in practice since their high reactivity typically leads to high burnout and lower carbon contents (LOI) relative to class F ashes as seen in Fig. 3.2.

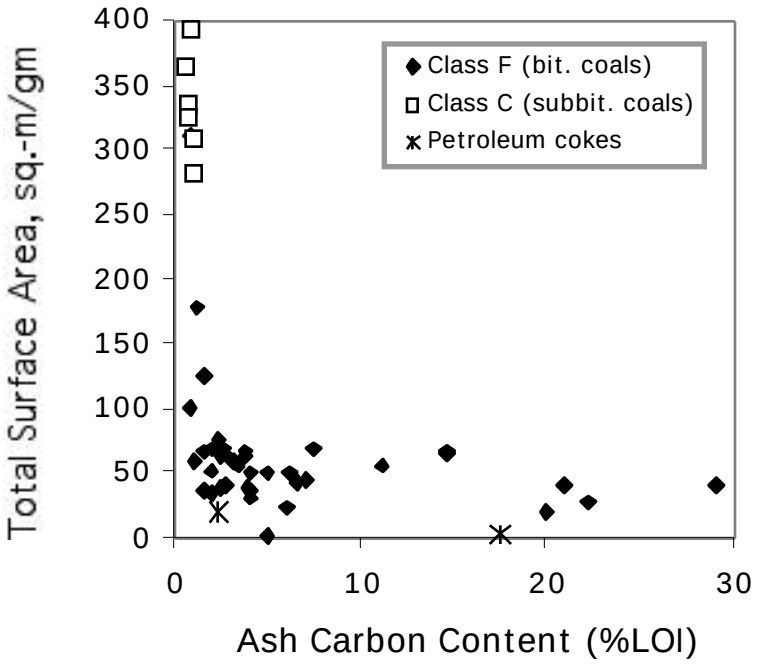

Figure 3.2 Surface areas of residual carbon in commercial ash samples determined by application of the BET theory to nitrogen adsorption isotherms at 77 K. The areas of the mineral portion of the ash were determined separately after oxidative removal of the carbon, and the values subtracted to isolate the specific carbon area. LOI is "Loss-on-Ignition" a standard approximate measure of carbon content in ash defined as the percentage mass loss during slow air oxidation at 750 ^{o}C.

Data from the laboratory portion of this study is summarized in Figs. 3.3–3.5 and Table 3.2. The high-heating-rate laboratory chars show total surface areas that increase monotonically with decreasing carbon content of the parent fuel. The surfactant adsorptivity shows a similar trend, increasing with decreasing carbon content from an immeasurably small value for petroleum coke to about 4 ml/g-carbon for the mid-rank coal char, but then decreasing to 1.7 ml/gm for the hard wood char. Fig. 3.4 shows that a better correlation is obtained when adsorptivity is plotted vs the surface area in pores larger than 2 nm determined by application of the BJH theory to the complete nitrogen isotherm. This is consistent with previous work on other carbon materials[3], in which it was shown that the utilization of micropores was incomplete in the standard surfactant adsorptivity test due to slow liquid phase diffusion of the large surfactant molecules[3].

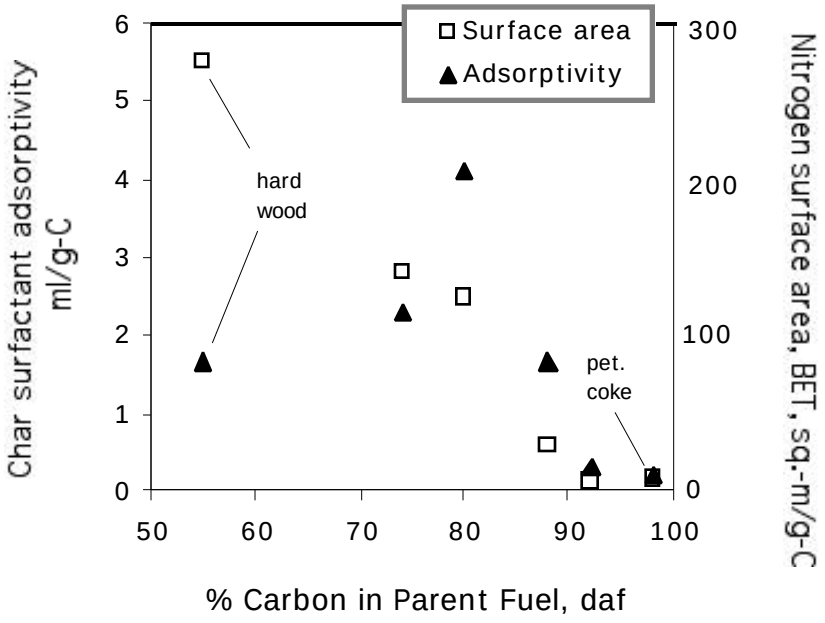

Figure 3.3 Surfactant adsorptivity and nitrogen BET surface area of various solid fuel chars (from upper portion of Table 3.1) prepared at high heating rates (~ $5 \cdot 10^4$ sec^{-1}) under standard conditions in a laboratory entrained flow reactor. Fuels are coals of various rank except where noted.

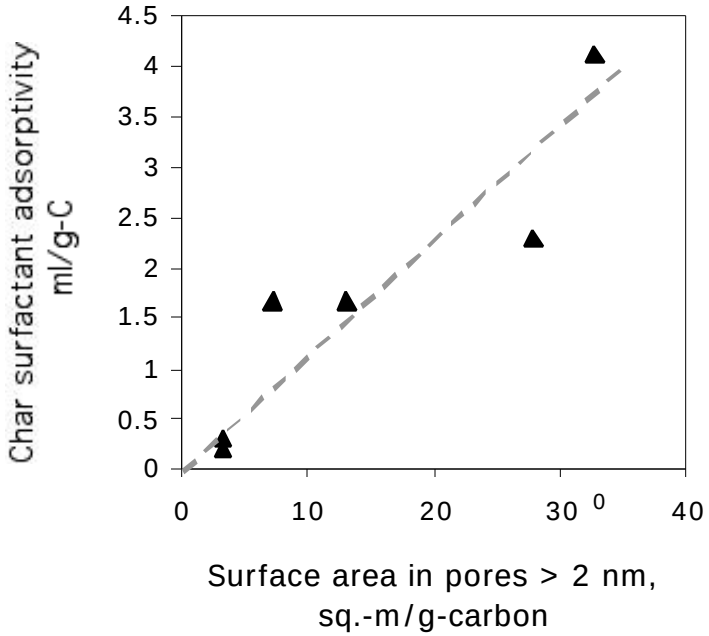

Figure 3.4 Surfactant adsorptivity vs. the sum of mesopore and macropore area (area in pores larger than 20 nm, from BJH theory applied to the nitrogen isotherm) in the laboratory generated chars from Fig. 3.3. Surfactant adsorptivity correlates better with this non-microporous area than with total surface area which is much higher in some char samples.

Table 3.2 and Fig. 3.5 present results on the effect of carbon surface chemistry. Oxidation by air at 440 ^{o}C or by ozone at 20 ^{o}C both decrease adsorptivity consistent with previous observations[10]. Data in Table 3.2 further demonstrate the reversibility of the process — heating to 1000 C to remove surface oxides recovers 80% of the adsorptivity (Table 3.2). It is difficult to characterize surface oxide groups by spectroscopic techniques in the presence of the abundant oxide minerals in ash. For this reason selected experiments were carried out on carbon black as a model carbon material with very low amounts of inorganic oxides. First Fig. 3.5 and Table 3.2 show that carbon black samples respond to surface oxidation in the same way as residual carbon — both air and ozone treatment decrease adsorptivity to much lower values. Secondly, XPS results in Table 3.2 show greatly enhanced atomic oxygen contents in the near-surface regions (penetration depth ~ 12 nm) of carbon black samples ozonated under the same conditions used for fly ash carbon. High-resolution spectral analysis of the high-binding energy tail of the C1s peak reveals increases in C-O, C=O, and O-C=O functionalities with only subtle differences between thermal (air) oxidation and ozonation.

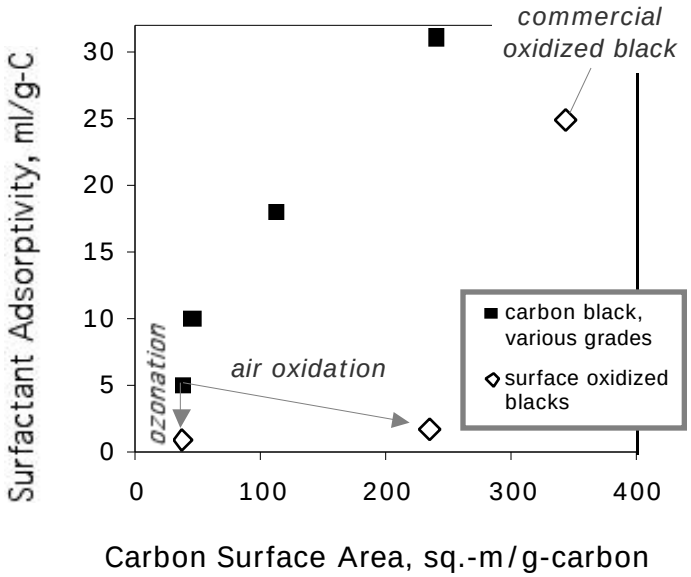

Figure 3.5 Effect of surface oxidation on total surface area and surfactant adsorptivity for carbon blacks as model materials. For carbon blacks, total area either increases or remains the same during oxidation, while surfactant adsorptivity decreases, a result that unambiguously identifies surface chemistry changes (rather than total area loss) as the primary mechanism of adsorption inhibition.

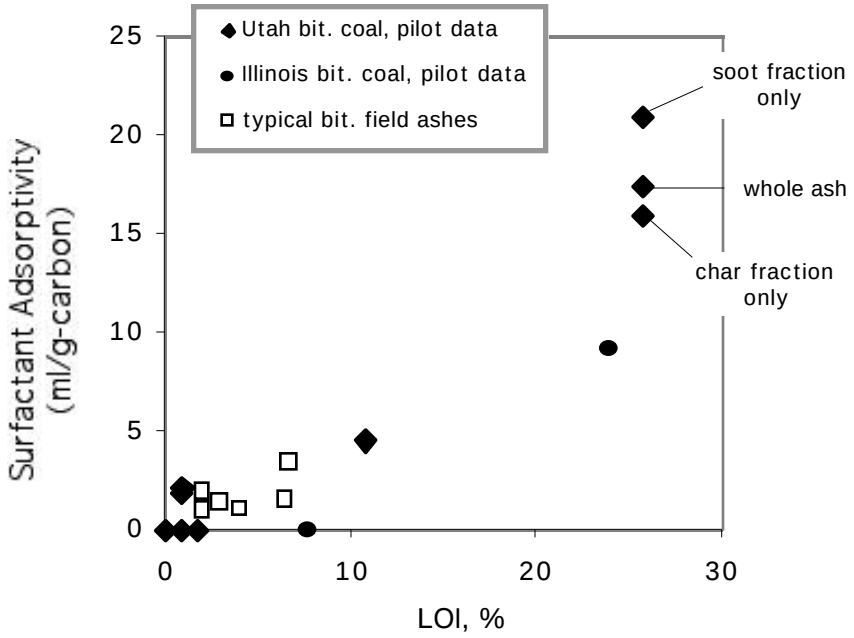

Figure 3.6 Pilot scale data on two coals burned in high-NO_x firing mode and in several different low-NO_x firing modes. As LOI (carbon content) of ash increases, the specific carbon activity toward surfactants also tends to increase. Separate contributions of soot and char from the highest LOI sample were determined using the fine particulate separation scheme of Veranth et al.[16].

The pilot-scale results are presented in Figs. 3.6-3.9 for a variety of low-NO_x and high-NO_x firing modes. Figure 3.6 shows that surfactant adsorptivity of the carbon residues from the U-furnace varies greatly, and tends to be higher for samples with poor burnout (high LOI). The combination of high LOI (gm-carbon/g-ash) and high specific adsorptivity (ml surfactant / g-carbon) makes the *total* adsorptivity of some of these ash samples (ml/g-ash) extremely high. The good superposition of data from commercial bituminous coal ash suggests that the U-furnace is a reasonable simulator of larger furnaces with respect to unburned carbon properties. Separation of char and soot from the very high LOI sample as described previously[17] shows that the fine carbonaceous fraction has a higher surfactant adsorptivity, though both the fine and coarse fractions contribute significantly.

Most of the high-LOI, high adsorptivity samples in Fig. 3.6 come from low-NO_x firing, but Fig. 3.7 shows that NO_x alone is <u>not</u> a good indicator of ash quality. In particular, low-NO_x firing modes can produce carbon with very high or very low adsorptive power. Figure 3.8 shows a good correlation between surface area and burnout (LOI) for the pilot-scale samples. Figure 3.9 shows a good correlation between surfactant adsorptivity and carbon surface area among the pilot-scale samples.

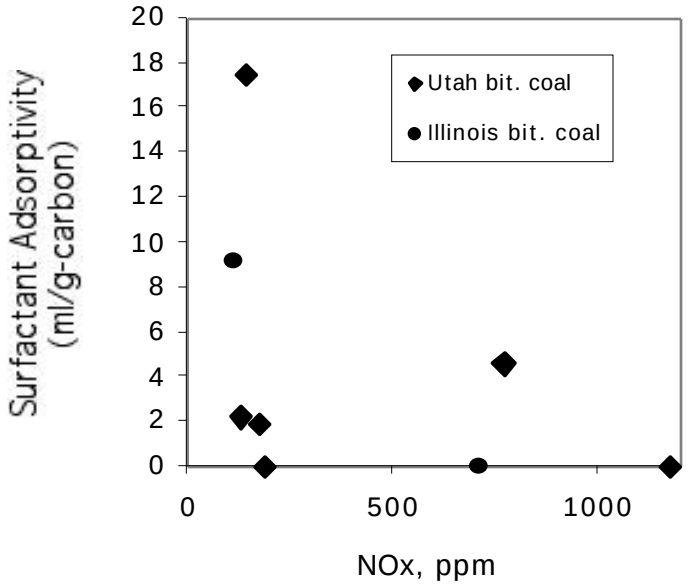

Figure 3.7 Pilot scale results giving residual carbon surfactant adsorptivity vs. NO_x at furnace exit. The low-NO_x carbons exhibit a wide range of activities making NO_x alone a poor indicator of carbon adsorptivity or ash quality.

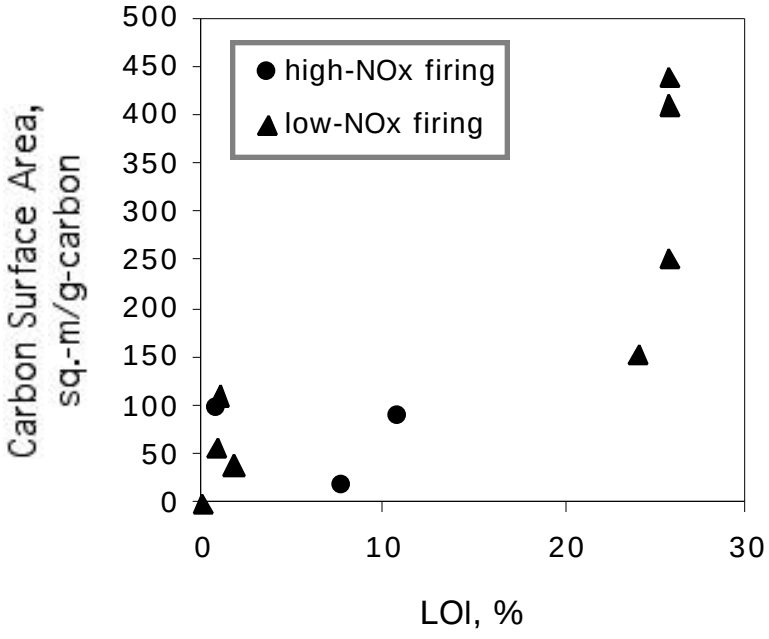

Figure 3.8 Pilot-scale results: residual carbon surface area (nitrogen BET) vs. ash carbon content (% LOI). Poor burnout (high LOI) generally leads to a high surface area residual carbon.

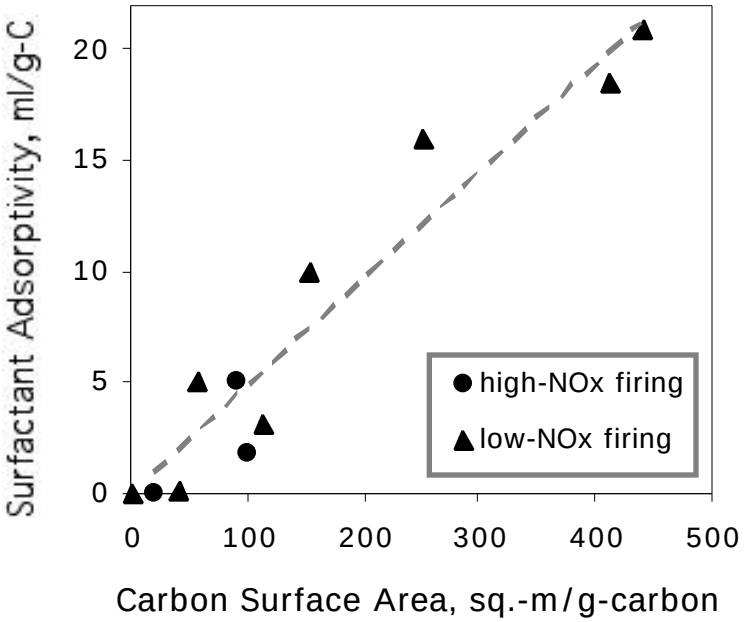

Figure 3.9 Pilot-scale results: residual carbon surfactant adsorptivity vs. carbon surface area (nitrogen BET). High surface area is the most important contributing factor to high surfactant adsorptivity (poor ash quality) in the pilot-scale samples.

Discussion

The present work establishes that unburned carbon properties are very sensitive to both fuel type and combustion conditions when care is taken to vary them independently. Because surfactant adsorptivity is the primary variable determining ash quality for concrete, we attempt to understand its behavior in detail below by separate consideration of three factors that co-determine its value: (1) carbon surface area, (2) accessibility of that surface for the large surfactant molecules, and (3) surface chemistry.

Carbon surface area. Residual carbon surface area decreases with increasing carbon content in the parent fuel, as expected, and also decreases with increasing burnout at the pilot-scale. This latter trend is consistent with decreasing surface areas during combustion at *high temperature* observed in several laboratory studies[2,14] and is the opposite of the behavior observed during *low temperature* combustion, which typically "activates" or increases the specific surface of carbon materials. The largest contributing factor to high adsorptivity among the pilot-scale samples is high carbon surface area (Fig. 3.9), which generally occurs in samples with poor overall burnout (Fig. 3.8).

Surface accessibility. The role of surface accessibility is illustrated by the improvement in the adsorptivity / area correlation when only mesopore and macropore area ($d_{pore} > 2$ nm) is counted (Fig. 3.4). It is also illustrated by the high specific adsorptivity of soot, whose area lies on the external surface of nanophase particles and is thus non-microporous and highly accessible. This argument based on soot structure is confirmed by the vapor adsorption data: the BJH meso- plus

macropore area of soot is 34.5 m^2/g, which is almost as high as the total BET area of 38.3 m^2/g indicating very little microporosity in soot and thus easy access by large surfactant molecules in solution.

Surface chemistry. The present data provide clear insight into role of surface oxides. First, the effect of ozone treatment is reversible when the samples are heated to a temperature sufficient to desorb the surface oxides (1000 ^oC). Secondly, oxidation of carbon black decreases adsorptivity dramatically while total surface area is constant or increasing. This observation resolves the question raised in earlier work[10] which was based solely on analysis of residual carbons. Residual carbons experience large decreases in total area during ozonation[10], making it unclear whether surface polarity or loss of total area is the dominant mechanism suppressing surfactant adsorptivity. In carbon black, however, the dominant meso- and macroporosity on the external surfaces of the nano-phase primary particles cannot be easily blocked by adsorbed oxides and thus total surface area is not lost during oxidation. Here the key role of surface *chemistry* is unambiguously established for the first time.

These combined results demonstrate that surface oxides, arising from combustion or from post-combustion treatment, make residual carbon surface less adsorptive and improve ash quality. The underlying mechanism in the aqueous concrete medium is depicted in Fig. 3.10 and described in the caption. Simple adsorption / desorption arguments suggest that the surface oxide population on carbon will vary with the combustion conditions, being lowest in hot, fuel-rich (reducing) zones which promote desorption, and highest during low temperature oxidation where an extensive stable oxide film builds up over the course of conversion[17]. Variations in native oxide content are thus believed to contribute to the observed variability in adsorptivity. Further, the hot, fuel-rich zones in low-NO_x environments have the potential to produce non-polar, high-adsorptivity carbon (see below).

Char Properties in Low-NOx Combustion

These results taken together provide new insight into the mechanism by which low-NO_x firing affects ash quality. Substantial field experience in North America has shown that installation of low-NO_x burners and/or overfire air ports for fuel staging increases unburned carbon levels and leads to field reports of poor air entrainment behavior in most cases. An important unanswered question is whether the degradation of ash quality is due solely to the increased carbon *content*, or whether chars exposed to fuel-rich zones in the near-burner region are also intrinsically "bad" (highly adsorptive). Data in Fig. 3.7 and 3.9 clearly show that some low-NO_x carbons are indeed intrinsically bad (have high adsorptivities per gram of carbon), but only those with poor overall burnout.

The following picture of low-NO_x carbon formation emerges from this study. The fuel-rich near-burner zones in staged firing delay char consumption and degrade burnout, but also drive off carbon surface oxides. If downstream mixing is incomplete, fuel-rich packets persist in which low-conversion, high-area, low-oxide-content char, and in some cases soot[16], are carried into the fly ash making it highly adsorptive and of poor quality for ash utilization. In contrast, a staged low-NO_x system with good downstream mixing reintroduces oxygen to the char surfaces, where it accomplishes further conversion, destroys surface area, destroys soot, and returns the pseudo-steady-state surface oxide population, effectively erasing the memory of the fuel-rich zone seen by the char surfaces in the near-burner zone. Thus low-NO_x ashes with good burnout (low LOI) are

observed to often possess benign (low-adsorptivity) carbon, as directly observed in the pilot experiments described herein.

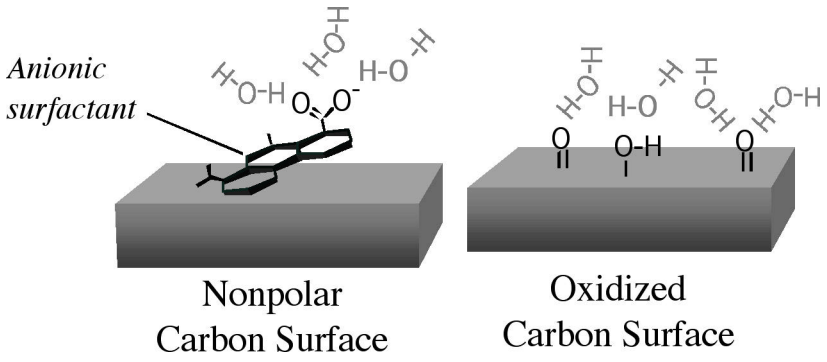

Figure 3.10 Sketch of aqueous phase interactions between concrete surfactants and carbon surfaces. Abietic acid anion is shown as a model compound representing the surfactant structures in concrete admixtures. The non-polar part of the surfactant molecule is shown adsorbing on the non-polar carbon surface(left), with which it interacts by dispersion forces, while the anionic part remains in aqueous solution. On polar carbon surfaces (right) these dispersion forces are too weak for the surfactant to displace water molecules, which have hydrogen bonded to surface oxide functionalities. Oxidation renders carbon surfaces hydrophilic — it is by this basic mechanism that air oxidation and ozonation decrease surfactant adsorptivity and improve ash quality for concrete applications.

Chapter 3 conclusions

1. Solid fuel selection strongly influences residual carbon properties, including surface area, surfactant adsorptivity, and oxidation reactivity.

2. Carbon surfactant adsorptivity, the most important ash quality variable in some regions of the world, is strongly dependent on combustion conditions, as determined through pilot-scale experiments in a single swirl burner facility operated in multiple firing modes on a given coal.

3. Surfactant adsorptivity is reduced by carbon surface oxidation occurring during combustion or during post-combustion treatment with air or ozone. Experiments on carbon black unambiguously demonstrate that increase in surface polarity and hydrophilicity is the governing mechanism.

4. Surfactant adsorptivity correlates much better with total burnout than with flue gas NO_x levels, indicating that low-NO_x chars are not all intrinsically "bad". Low-NO_x flames can produce low-adsorptivity chars and high quality ash for utilization, provided downstream temperatures and secondary/tertiary air mixing are favorable for overall burnout. This result is encouraging for ash utilization from low-NO_x technologies.

References for Chapter 3

1. Helmuth, R. *Fly Ash in Cement and Concrete*, The Portland Cement Association, Skokie, Illinois, 1987.
2. Hachman, L., Burnett, A., Gao, Y., Hurt, R.H., and Suuberg, E.M. *Proc. Comb. Inst.* 27:2965 (1998).
3. Yu, J., Külaots, I., Sabanegh, N., Gao, Y., Hurt, R.H., Suuberg E.S., and Mehta, A., *Energy and Fuels*, 14:591 (2000).
4. Hill, R.L., Sarkar, S.L., Rathbone, R.F., and Hower, J.C., *Cement and Concrete Research* 27:193 (1997).
5. Pedersen L.S., Glarborg P., Dam-Johansen K., Hepburn P.W., and Hesselmann. G., *Comb. Sci. Tech.* 132:251(1998).
6. Cloke M., Lester, E., and Gibb, W. *Fuel* 76:1257(1997).
7. Walsh, P.M., *Energy and Fuels*, 11:965 (1997).
8. Maroto-Valer, M.M., Taulbee, D.N, and Hower, J.C. *Fuel* 80:795 (2001).
9. Ban, H., Li, T.X., Hower, J.C., Schaefer, J.L., and Stencel, J.M. *Fuel* 76:801(1997)
10. Gao, Y., Külaots, I., Chen, X., Aggarwal, R., Mehta, A., Suuberg, E.M., and Hurt, R.H., *Fuel* 80:765 (2001).
11. Maroto-Valer, M.M., Zhang, Y.Z., Andresen, J.M., Jones, A., and Morrison, J.L., *Am. Chem. Soc. Div. Fuel Chem. Preprints* 221:115 (2001).
12. Kualots, I. Ph.D. Thesis, Division of Engineering, Brown University, May, 2001.
13. Veranth, J.M., Pershing, D.W., Sarofim, A.F., and Shield, J.E., *Proc. Comb. Inst*. 27:1737 (1998).
14. Davis, K.A., Hurt, R.H., Yang, N.Y.C., and Headley, T.H., *Comb. and Flame* 100:31 (1995).
15. Charpenay, S., Serio, M.A., and Solomon, P.R., *Proc. Comb. Inst.* 24:1189 (1992).
16. Barrett, E.P., Joyner, L.G., and Halenda, P.P., *J. Am. Chem. Soc.*, 73:373 (1951).
17. Veranth, J.M., Fletcher, T.H., Persing, D.W., and Sarofim, A.F., *Fuel* 79:1067 (2000).
18. Lizzio, A.A., Piotrowski, A., Radovic, L.R., *Fuel* 67:1691 (1988).

Chapter 4 Critical Examination of the Foam Index Test

Introduction

At the present time, a large amount of coal fly ash is utilized worldwide as an additive to concrete. Not only does this use solve an ash disposal problem, but it also results in an improvement in concrete product properties (additives that serve this purpose are termed pozzolans). The suitability of a particular fly ash as a pozzolanic additive to concrete, however, depends upon several factors related to the unburned carbon content of the fly ash. It is the carbon's porous surface area which is important in determining the capacity of the carbon to adsorb air entrainment admixtures (AEAs) [1-3]. The AEAs are surfactants added to concrete in order to create fine air bubbles (<1 mm diameter) during the mixing of the concrete, hence the origin of the term "air entraining agent". These air bubbles impart freeze-thaw resistance to the concrete by providing void volume to accommodate expansion of residual water during freezing. When a fly ash contains a large amount of carbon, the adsorption of the AEA surfactant by the carbon destroys the ability of the concrete to hold the required air. It is this adsorption problem that dictates the rejection of large amounts of commercial utility ash. The ability of the carbon to adsorb AEA depends upon not only its surface area, but also the accessibility of that area and its polarity [3], factors that are well-known in activated carbon design. Recognition of this has led to the identification of ozonation as a tool for rendering ash carbon surfaces polar and thus of lower AEA adsorption capacity [4].

One of the key requirements for systematic design of activated carbons is that certain well-defined benchmark tests be available for evaluating the carbons. The same is true in evaluating the suitability of a fly ash as a pozzolan, or for designing AEA adsorption mitigation procedures. Historically, the well-known "foam index" test has served this purpose. Unfortunately, this is not a standardized test and different laboratories have used widely different procedures. Moreover, there are a great many candidate commercial AEAs that can be used for the test. Thus there has never been good comparability of results from lab-to-lab, or even within a single lab, if the AEA supply is changed.

It has also been recommended by an ASTM task group that an improved foam index method be developed [5]. While this report does not touch upon all aspects of those recommendations, it offers some insights into some aspects of the problem, and provides what is a step in the desired direction.

In this report, we present research on several chemically pure candidate surfactants tested against commercial AEAs, utilizing many commercial utility ashes from the Brown University ash sample bank. These easily obtained pure chemical surfactants offer the opportunity for development of a standardized foam index test that can allow true inter-laboratory comparisons. Development of a standardized test using a spectroscopic assay of AEA adsorption, as has been recommended [5] would likewise benefit from use of a pure surfactant. While spectroscopic methods have already been utilized in examining adsorption of commercial AEA materials [6,7], there remains the concern that with the mixed commercial materials, there may be differences in how different fly ashes adsorb different components from the mixtures. If different components have different light absorbing characteristics, then there could develop uncertainties in calibration. For example, if an AEA were to contain one strongly and one weakly light absorbing component of comparable surfactant strength, and if one fly ash preferentially adsorbed mainly the first, while the second adsorbed mainly the second (as could happen for reasons of molecular accessibility of surface character), then the light

absorption would characterize the AEA capacities as very different while the foaming behavior could be similar. To avoid any such issues, it would appear better to develop a spectroscopic test with a pure material that would at least serve as a reference for further testing with actual commercial mixtures.

Experimental

Air Entraining Admixture and Surfactant Materials

The commercial AEAs that were examined as part of this study were Darex II™ (provided by W.R. Grace and Co. of Cambridge, Massachusetts) and Air 40™ (from Boral Material Technologies, Inc.). Darex II is described by its manufacturer as a "complex mixture of organic acid salts". It is a non-vinsol product, just as is the Air 40 which is formulated with a "stabilized modified resin surfactant", according to its sales literature.

The candidate pure surfactant materials were sodium dodecyl sulfate (SDS), abietic acid sodium salt (AAS) and dodecyl benzenesulfonic acid sodium salt (DBS). All of these have either been used or considered for use as actual air entraining agents [8]. None of them, are however, in common commercial use in standard fly ash concrete, for reasons of performance and especially, expense. They do, however, closely mimic the behavior of the commercial anionic-type AEA compounds under the usual foam index-type test conditions, as will be presented below. The SDS (MW=288 g/mol) and DBS (MW = 348 g/mol) were purchased in commercial reagent grade, while the AAS (MW = 324 g/mol) was prepared in-house from commercial reagent grade abietic acid.

Fly Ash and Cement Samples

A total of 29 fly ashes, including both class F and class C samples, were selected for various aspects of the testing program. The samples were chosen from the Brown University coal fly ash sample bank of roughly 80 fly ashes. These samples have been obtained from utilities (or ash brokers) throughout the U.S. The class F ashes are formally characterized by an inorganics content of (SiO_2 + Al_2O_3 + Fe_2O_3) which is no less than 70%, whereas the class C ashes must contain only more than 50% by weight of these components [9]. The difference between the two classes is associated with the higher alkali and alkaline earth contents of the class C ashes. This classification generally places the ashes from bituminous coals and anthracites into class F and those from lignites and subbituminous coals into class C.

The actual samples used in this study are shown in Table 4.1. The particular utilities and units that produced the samples are not specifically identified, because not all samples are fairly representative of their current "normal" practices. All samples were, however, produced in full scale boilers under actual load conditions.

The cements used in the foam index testing work were all standard commercial Portland cements, purchased from local hardware dealers. There was some variability in the results of foam index testing performed on different cements. For this reason, it was important to perform a "blank" experiment with each cement, as part of routine foam index testing. This will be discussed further below.

Table 4.1. The Fly Ash Samples Examined

Sample Number	Class	LOI (%)	BET Area (m^2/g-C)
1	F	6.5	43
3	F	14.6	65
4	F	14.6	65
6	F	3.4	57
10	F	2.6	66
21	F	6.1	51
23	F	65.5	54
25	F	2.5	39
26	F	4.0	33
39	F	0.8	312
40	C	1.1	282
41	C	1.1	309
42	C	0.6	238
43	C	0.6	365
44	C	0.6	326
45	C	0.7	335
46	F	11.2	56
49	F	19.9	20
50	F	22.2	28
51	F	20.9	41
53	F	4.0	50
57	F	0.8	102
61	F	1.6	38
63	F	7.1	45
64	F	7.4	69
65	C	0.7	326
68	C	0.8	326
74	F	9.8	63
75	C	1.3	377

Loss-On-Ignition Measurements and Surface Area Determination

The adsorption of surfactant is associated with the presence of unburned carbon in the ash. The test that is normally utilized for determining unburned carbon content is the "Loss-on-Ignition" (LOI) procedure. These tests were performed on 1 gram samples, pre-dried in a laboratory oven at 130°C for two hours. After drying, cooling and re-weighing, the samples were placed into an air ventilated laboratory oven at 740°C for two hours, in order to burn out the residual carbon. The loss in mass at 740°C was reported as the LOI, and this is assumed to be the weight of unburned carbon in the original sample (though there is a possibility of a small amount of contribution from some slow mineral phase decomposition reactions [10],.

Surface areas of the samples were determined using nitrogen in an automated Autosorb 1 gas adsorption device from Quantachrome, Inc. Standard BET analysis procedures were employed.

Foam Index Test

The foam index test is the commonly employed field test for determining the suitability of a particular fly ash as a concrete additive. Again, it is carried out in different ways by different groups, and there is no true standard methodology. The purpose of the test is to determine what is equivalent to a titration endpoint for adsorption of an AEA on a particular ash. The ash is contained in a simulated aqueous concrete mixture, which is somewhat thinner in consistency than an actual concrete mixture (in order to ensure good mixing). When the ash in the mixture has adsorbed an amount of AEA needed to fully saturate all *accessible* adsorption sites, "normal" surfactant behavior can be observed in the water phase, i.e., the test solution supports a stable foam on its surface. Generally speaking, the more surfactant that is needed for titration to the foam index endpoint, the poorer the performance of the ash is likely to be in the field. The test is very widely used because it can be performed in the field and involves no special equipment.

Different AEAs can give quite different values of the foam index, which is one reason why it is difficult to develop a truly standard test. The difference in performance has to do not only with the chemical nature of the AEAs (which may be derived from a variety of natural and synthetic sources), but also with their aqueous concentrations.

In the present work, the foam index tests were based upon commonly used procedures [11,12], but with details determined by local circumstances, as is generally the case. The testing involved placing two grams of fly ash, 8 grams of Portland cement and 25 ml of deionized water into a 70 ml, 40 mm I.D. cylindrical jar. The jar was capped and thoroughly shaken for one minute to completely wet the cement and ash. A 10 vol.-% aqueous solution of commercial AEA was then added one drop (0.02 ml) at time from a pipette gun. Following addition of each drop the jar was capped and shaken for approximately 15 seconds, after which the lid was removed and the liquid surface observed. Before the endpoint of the test, the foam on the liquid surface was unstable, quickly breaking and disappearing from the free surface. The endpoint was taken to occur when foam remained stable on the surface at least 45 seconds. As noted above, a blank value was measured using only Portland cement in water. Subtraction of the blank value from the actual test results gave the reported foam index value for the fly ash (in ml, per two grams of ash). All foam index tests were replicated at least twice, and the reported values are averages of the replicates.

The same procedure was used with the pure surfactant materials, though the solution concentrations were varied so as to provide values in an easily measurable range. The actual concentration values will be given below.

It is important to note that the foam index test is a *dynamic* test, as opposed to an equilibrium measurement. It has been reported elsewhere [6] that the full equilibrium adsorption of surfactant by fly ash is characterized by timescales on the order of hours, as opposed to the timescale of the foam index test, which is minutes. Though this finding has recently been challenged, based upon results suggesting that the equilibration time might be ten minutes or less [7], it is believed that this could depend somewhat on the nature of the carbon in the ash. Regardless of which timescale is correct, there is general agreement that the dynamic nature of the commonly utilized foam index procedures could lead to an underestimate of actual long-time equilibrium uptake of AEA by fly ash carbon. This can help explain why in the field, it is observed that a load of concrete that appears to

have proper dosing of AEA, based upon the foam index test, can sometimes go "flat" (lose its air content) during transport to a job site. This issue was not further considered in this work, except as noted below.

Results and Discussion

Correlation of Foam Index Results Using Different Commercial AEAs

Both the Darex II and Air 40 are widely used commercial AEAs, which are derived from natural materials, and as earlier noted, have complex and not easily characterized, compositions. One of the first issues addressed in this work was whether these different commercial AEA products behaved similarly, when tested under comparable conditions. If two common commercial materials do not show some degree of correlation in behavior, there would be little hope of developing a foam index test based upon pure surfactant models. Because of the wide variety of different types of materials used for preparation of commercial AEAs, a more extensive test matrix, comparing different agents under controlled conditions, would be useful for establishing the generality of the present results. Still, the results to be presented below, from work involving different kinds of model surfactants, provide confidence that a very wide range of commercial materials will behave in a similar manner.

An arbitrary choice was made to perform the foam index test using the commercial products at 10% volume dilution, in deionized water. Since the AEA products are aqueous solutions, as shipped, the addition of pure water is not expected to change their character. In any event, in actual use the solutions are diluted to an even greater degree in the concrete mixture. The dilution of the as-received AEA allowed a convenient number of drops to be utilized in the foam index test procedure described above.

The absolute concentrations of the surfactant compounds were probably not the same for the two commercial AEA solutions. In a test involving drying of the solutions in a vacuum oven, the Air 40 gave approximately 20% greater non-volatile residue than did the Darex II. No further effort was made to characterize the AEAs in detail, and this 20% difference in residues does not necessarily reflect the difference in actual surfactant concentrations in the two AEAs.

It was observed that the foam index results using Darex II and Air 40 were well correlated with one another, for the particular subset of ashes chosen for testing. The results are shown in Figure 4.1. It should be recalled that a difference of 0.02 ml is equivalent to a single drop uncertainty in determining the endpoint of the test. The results seemingly imply that the Air 40 solution is roughly three times "stronger" than the Darex II solution, but again, the concentrations used for this test are arbitrarily set. The results of Figure 4.1 gave confidence that the performance of commercial AEAs from different sources can be reasonably correlated with one another.

3.2 The Problem of AEA "Aging"

There was a very obvious "aging" of the commercial AEAs. Over the course of several weeks, the foam index of a "standard" ash sample increased measurably, if the same batch of prepared 10% AEA was utilized. Both the Darex II and Air 40 showed the same qualitative trend. The trend could apparently be retarded by storing AEA solutions in a tightly stoppered vessel from which light was excluded. This was suggestive that the aging involved oxidation of the AEAs, but the question was not pursued further here.

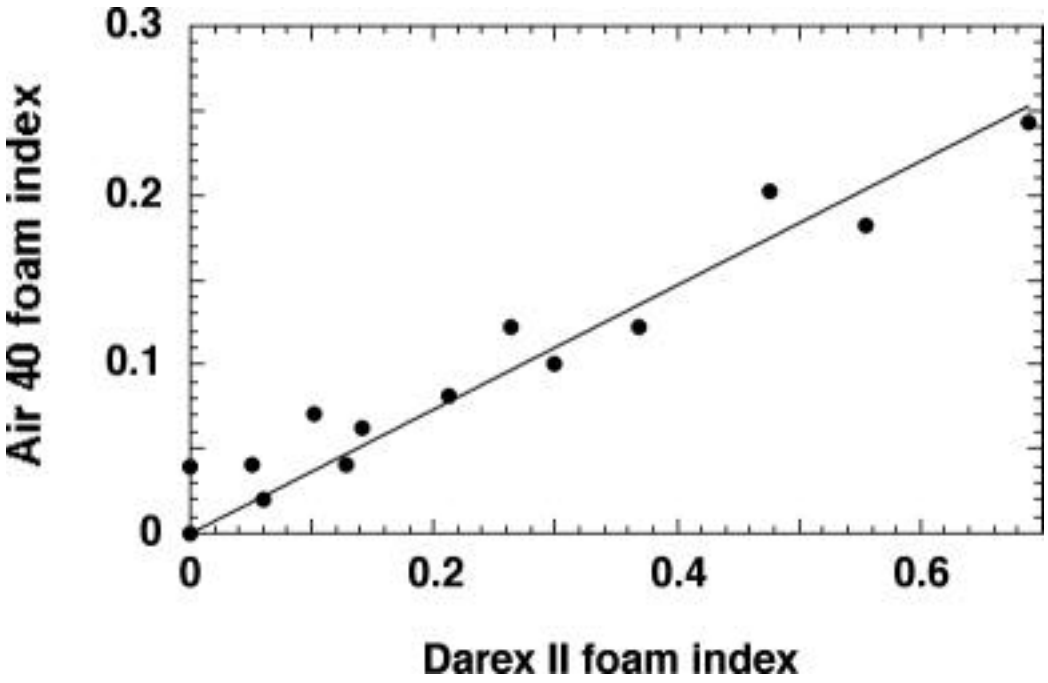

Figure 4.1 Comparison of foam index measured with Darex II 10% solution vs. that measured with Air 40, 10% solution. The fly ashes used in this comparison were numbers 1, 4, 10, 21, 39, 49, 50, 51, 53 57, 61, 63 and 64.

A recent paper [7] has offered that there could be a role of carbon dioxide absorption in changing the character of an AEA solution. This was attributed to a change in the pH of the solution, and the formation of free acid from the original salt form, leading to surfactant precipitation. Oxidation processes can also lead to formation of additional organic acids, in addition to those from the carbon dioxide absorption route. Whatever the mechanism, the use of commercial AEA materials for routine foam index testing carries with it some danger of unanticipated change of composition.

Thus another advantage in the use of freshly prepared pure surfactants for foam index testing is that changes in the foam index obtained with the pure reagents will be more reliably indicative of changes in the fly ash, as opposed to an artifact of the change in the AEA itself.

The Role of Carbon in Adsorption

It has recently been suggested that the carbon in fly ash might be unable to adsorb AEA on the timescale of the foam index test [7], and that this leads to greater importance of faster adsorption processes on mineral or inorganic fractions of the ash. The results of the present testing program do, however, support the key role that carbon plays in the present foam index testing program. Other papers have presented evidence of the important role of carbon [1-3], and it would be difficult to rationalize the effect of ozonation treatment on fly ash foam index [4], but for the role of carbon in adsorption.

Here, the results of two additional experiments directly supported the role of carbon adsorption in foam index testing. Samples of fly ashes 21 and 39 were subjected to foam index testing, following

the LOI determination procedure described above. The samples tested in this way were therefore carbon free, but the inorganic portion should be essentially unchanged (the laboratory oven operates at a temperature much lower than the samples "saw" in the boilers). In the case of fly ash 39 (starting LOI = 0.8%), the foam index with Air 40 decreased from 0.06 to 0 and in the case of fly ash 21 (starting LOI = 6.1%), the foam index with Darex II decreased from 0.3 to 0. Thus in the foam index testing as performed here, the carbon is the primary variable that determines the foam index values.

Effects of Ash Sample Amount

The foam index test can be quite tedious in the case of samples containing large amounts of unburned carbon (high LOI). If the drop size is kept small, in order to maintain accuracy at the endpoint, quite a large number of drops are required to reach the endpoint with a high LOI sample. Inasmuch as each drop addition is associated with 15 seconds of agitation, followed by examination of the foam, the testing time can become quite long for such high LOI samples.

As already noted, the foam index value is a result of a dynamic measurement, as opposed to an equilibrium measurement. If the procedure is changed so as to introduce a large initial aliquot of AEA (to quickly get near to the endpoint of the titration), the time of testing can be shortened. This, however, means that the time available for equilibration of the mixture is also shortened. The endpoint of the foam index test depends purely upon the aqueous concentration of the AEA, which can be taken as a constant value. A shorter test time means that adsorption on the solid is less complete when the required aqueous endpoint concentration is achieved, because of the finite kinetics of adsorption from solution (most likely dictated by diffusional kinetics). It was indeed observed that addition of a large initial aliquot of AEA gave lower foam index values than when the dropwise addition procedure was followed.

In certain types of AEA adsorption testing, gradual atmospheric carbon dioxide dissolution into the test solution can also influence results [7]. In the present study, this was of limited concern because there was always a high pH maintained in solution, due to the presence of a large amount of cement in the mix. This would easily overwhelm any small amount of carbon dioxide absorption that might occur during the test (the pH of saturated calcium hydroxide or carbonate solutions in equilibrium with atmospheric carbon dioxide is still basic). Because the procedure used in [7] did not include cement in the mix, there would have been a greater sensitivity to carbon dioxide absorption in that work. Thus we believe that the time dependence of foam index values in the present study does have to do with finite adsorption times of AEA onto carbon.

In an attempt to avoid use of a large number of drops during high LOI ash sample testing, another modified foam index procedure was developed. This simply involved reducing the amount of ash from the "standard" two gram amount to something lower, but then back-calculating the foam index results to an equivalent two gram of ash basis. The results of such experiments are shown in Figure 4.2. As the sample mass was reduced to small values the (back-calculated) foam index often became quite large. The behavior was not consistent from sample-to-sample. Ashes with higher LOI values seemed to require a greater amount of sample in order to achieve an asymptotic value, characteristic of the standard procedure.

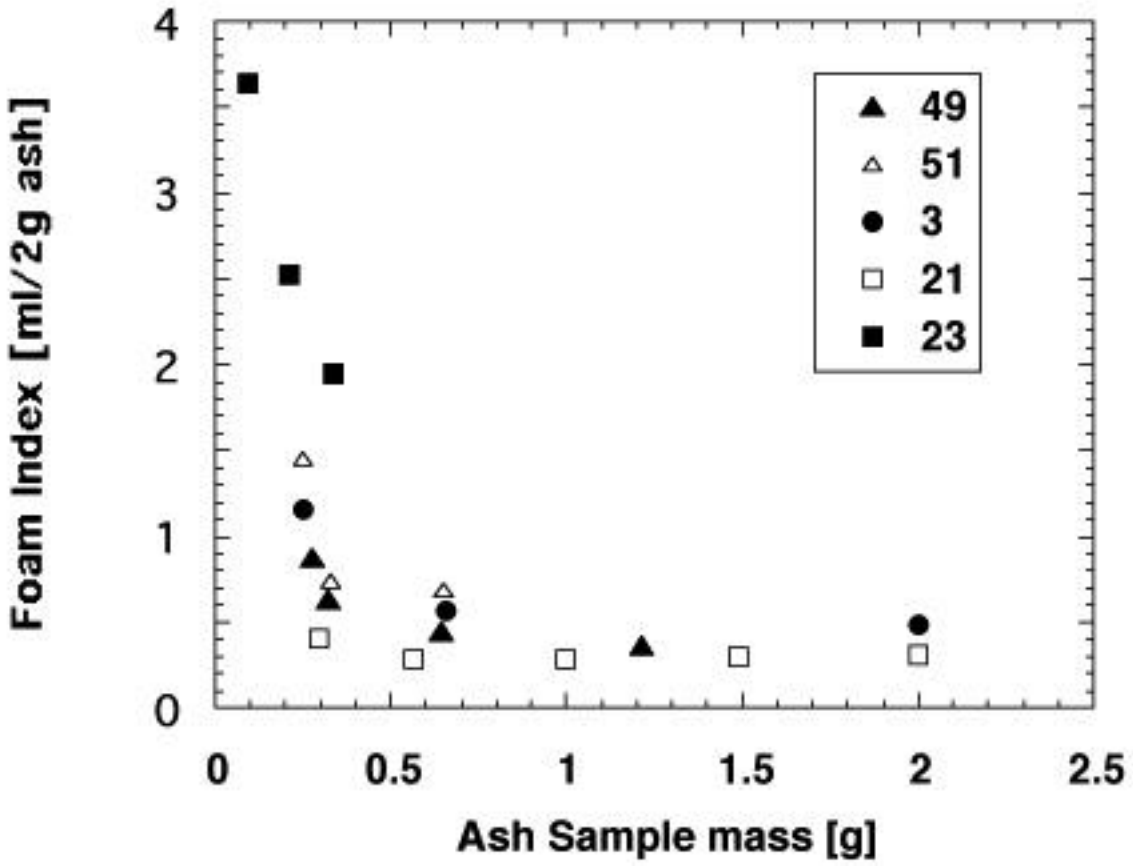

Figure 4.2 The influence of amount of fly ash on apparent foam index, for Darex II. The amount of cement and water were kept constant for all of the tests.

The results of Figure 4.2 cannot be explained by the dynamic nature of the test, discussed above. The time for adsorption onto any particle of carbon should independent of the total amount of ash sample that is tested. Since the time to reach the the foam index endpoint is shorter the smaller the amount of sample, the time available for AEA adsorption onto the carbon decreases with sample amount. This should lead to a *lower* apparent foam index for small amounts of sample (when calculated to the two gram basis), opposite the observed trend. Consequently, the explanation for the dependence of foam index results on ash sample amount must instead be associated with changes in some mixture characteristics, related to the addition of differing amounts of ash to the testing mixture.

The most obvious possibility involves water-soluble inorganics in the ash. When a very high carbon ash (such as 23) is tested, adding a small amount of this ash adds very little mineral matter, and hence, soluble components. This is why the increase in foam index with decreased amount of sample is so notable in that case. Based upon present results, a minimum of at least 0.3 g of actual ash mineral had to be added to the test mixtures, in order to begin to see the asymptotic behavior.

The ash contributes soluble components to the testing mixture. It is possible that alkali components are responsible, since it is well established that increases in alkali content increase air entrainment [8,11,13,14]. An increase in foaming efficiency, as is associated with better air entrainment, would be

correlated with a decrease in foam index. High concentrations of monovalent alkali cations assure good surfactant behavior whereas divalent alkaline earth cations reduce the efficiency of AEA surfactants by a precipitation mechanism, well known as the "hard water" problem [7, 11].

Because the introduction of ash to a testing mixture adds a number of soluble compounds, it is difficult to state with any certainty from these experiments which soluble components were the most critical. For this reason, a separate testing program was conducted, involving pure additives and commercial AEA solutions, in order to determine which soluble inorganic species might influence foam index values.

Influence of Solution Chemistry on Foam Index

These tests were all carried out using 25 ml of deionized water, to which were added various salts. The foam index procedure was then followed, in this case without the addition of any cement or actual ash, except as noted. Both the Darex II and Air 40 were examined and always gave the same behavior, though the numbers of drops required for stable foam formation were always different. Darex II is a near-neutral water solution, whereas Air 40 is basic in character. This difference in starting characteristics had no apparent effect on the behavior observed in the following tests.

It should be noted at the outset that performing the foam index test with deionized water yielded no foam endpoint. This is presumably because the tested solutions became acidic, due to absorption of atmospheric CO_2 [7]. The solutions had a cloudy character, as the surfactant precipitated in the expected manner.

Addition of just two grams of cement to deionized water reduced the AEA requirement for foaming to a few drops, just as in the case of the normal foam index "blank". Addition of a few grams of carbon-free ash, prepared by completely burning out the carbon in a laboratory oven, also reduced the foam index "endpoint" to a few drops of 10% solution. Both these additions resulted in the solution becoming basic (the cement more so than the ash mineral). The solution pH was believed to be an important factor in foam development. This was explored using different alkali solutions.

Addition of NaOH to pure deionized water (pH =13) resulted in a foam endpoint comparable to that with mineral or cement, but if the NaOH was neutralized by addition of $CaCl_2$, again no stable foaming behavior was observed. Addition of neutral salts such as Na_2SO_4 or NaCl, or acidic salts such as $CaCl_2$ to deionized water did not yield any foaming behavior when tested with the AEA. Thus solution pH was shown to be important for developing the surfactant behavior, as expected, and the presence of monovalent alkali alone was not sufficient to create foaming action if the solution was not basic.

On the other hand, addition of 0.1 g of pure $Ca(OH)_2$ yielded a solution of high pH (12.8), but did not give a good, stable foam, even upon addition of a large number of droplets. This is presumably a consequence of insoluble complexing behavior with the calcium ion, also in agreement with the results of another study [7]. Thus high pH alone does not necessarily lead to good foaming behavior. When the amount of $Ca(OH)_2$ was increased to 1 g, the solution was saturated and took on a milky white appearance, as opposed to the clear appearance of the true solution obtained with the lesser amount of $Ca(OH)_2$. In this saturated solution case, a stable foam could be obtained, though only with a large number of drops.

Addition of alkali carbonates (Na_2CO_3, K_2CO_3) to deionized water led to stable foam formation upon addition of only a few drops. This is not surprising, in terms of the pH effect of the carbonate ions, and the fact that monovalent cations (Na^+ and K^+) were involved. These conditions together favor the usual foaming action of the surfactant. On the other hand, addition of divalent carbonate salts ($CaCO_3$ and $MgCO_3$) led to mixed results. The magnesium and calcium carbonate were expected to give poor foam formation and stability, because of the usual divalent cation effects. This was observed to be the case for magnesium, but surprisingly not for the calcium.

One particular sample of extremely finely divided $CaCO_3$ gave a stable foam immediately upon mixing, whereas a solution prepared from a more coarse $CaCO_3$ did not. The calcium carbonate has extremely low solubility, and in both cases the solutions were saturated. The more finely divided calcium carbonate provided an equilibrium (saturated) solution more quickly than could the coarser powder, based upon pH measurements of the solutions. Once the equilibrium pH (around 8.4, as expected for solutions in contact with air) was established, both calcium carbonate samples gave foam index endpoints that were very similar to those obtained with monovalent cation carbonates or cement. This result was not anticipated, as the usual "hard water" precipitation of surfactant had been expected. It has, however, been reported that the calcium surfactant salt precipitates can readily redissolve in such solutions, maintaining an equilibrium ionized surfactant concentration [15]. This is indeed why air entrainment is possible, despite the high dissolved calcium content of concrete mixtures.

In a separate experiment, a solution was again prepared with calcium hydroxide and tested with AEA (Air 40), yielding, as usual, no stable foam endpoint. This mixture of water, $Ca(OH)_2$ and AEA then had a few hundred milligrams of the finely divided calcium carbonate added, and was agitated. A stable foam was again immediately achieved with no further addition of AEA. In this experiment, the solution was always basic and always contained calcium ions. The difference in foaming behavior was associated with the introduction of the carbonate to the mixture. The earlier results with magnesium carbonate had demonstrated that improved foaming was not directly associated with addition of the carbonate ion, per se. In fact, the presence of a high concentration of calcium hydroxide would tend to greatly limit the solubility of the carbonate in solution, so it was unlikely that a solution equilibrium was being affected through dissolution of carbonate. These results, as well as the earlier described results with saturated $Ca(OH)_2$ solutions, suggested an alternative explanation. It appears that the presence of finely divided undissolved solids is beneficial to surfactant foaming behavior, possibly through a mechanism of adsorption of calcium surfactant species onto the surfaces of the solids [15]. This possibility received some support from the observation that there was an effect of the amount of finely divided calcium carbonate on foaming (addition of more of the finely divided carbonate induced foaming more readily). Because these amounts were always well above those needed for saturation of calcium carbonate solution, the effect could not be associated with contributions to solution from dissolution of the powder. The ability to produce a stable foam depends somehow on the available surface of undissolved carbonate or hydroxide particles. This is why the coarse calcium carbonate powder was initially ineffective at inducing foaming action, and only slowly approached the finely divided powder in efficacy over time.

The foam index of an ash tested in solution together with pure finely divided $CaCO_3$ was the same as that when the ash was tested with the normal amount of cement. The behavior was no different

than when the ash or calcium carbonatewere tested alone. Addition of $Ca(CO_3)$ to a solution of $Mg(CO_3)$ again very quickly provided the latter the ability to develop a stable foam, despite the fact that the $Mg(CO_3)$ solution was by itself completely unable to support a foam.

The above results have made a strong case for the importance of finely divided calcium powders in providing foaming action, in solutions that might otherwise be unable to support foaming action. In the normal foam index test, the cement powder clearly provides this function. To the extent that related behavior has been observed before, in different kinds of experiments [15], the result is not surprising.

The above results, together with others recently published [7], thus confirm the importance of aqueous medium in the foam index test. Different choices have been made by us and by others [7], with regard to the addition of cement to the test mixtures; we have chosen to add cement to the mixtures. Addition of cement of course makes the performance of spectroscopic measurements, such as have been of recent interest [6,7] very difficult. On the other hand, the presence of cement assures the existence of an aqueous medium much more representative of the actual concrete mix. The presence of a high concentration of cement in the mixture eliminates concerns about the effect of CO_2 dissolution during testing [7], as it serves as an excellent alkaline "buffer". It also provides the finely divided calcium solids that appear to be important. The question of the mechanism by which finely divided calcium solids influence the foaming behavior was not pursued further here. It can, however, be noted that the testing work with pure surfactant materials proved much less sensitive to such additive effects (see below).

Alternative Surfactants for Foam Index Testing

Three alternate surfactants were examined, SDS, DBS and AAS. The foam index test procedure with all three of these surfactants was the same as it was for the commercial AEA materials.

In the case of the SDS, the surfactant was prepared into a 1wt. % solution (approx. 0.035 M), using deionized water. Results for a series of typical ashes are shown in Figure 4.3, in comparison with the results using Darex II on the same ashes. It should be noted that the actual mass of Darex II in solution was quite comparable to the mass of SDS in solution. The SDS is quite clearly a much stronger surfactant, as less SDS is required to reach a stable foam endpoint, compared to Darex II.

An AAS solution was prepared by dissolving pure abietic acid into water, and then reacting with a stoichiometric amount of sodium hydroxide. The resulting solution was 0.05 M. The behavior of AAS against Darex II was qualitatively similar to that already reported for SDS, but the required volume to reach the endpoint was quite a bit higher (see Figure 4.3).

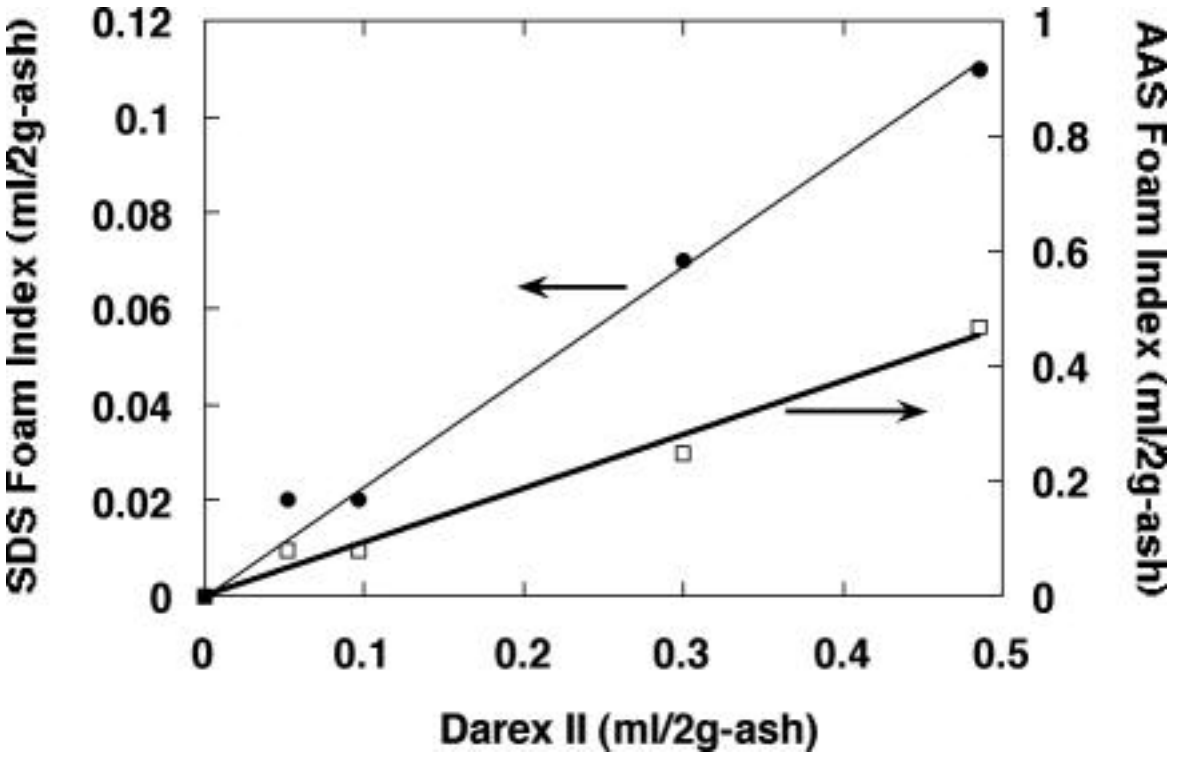

Figure 4.3 A comparison of the foam index determined using SDS and AAS, versus the foam index using the Darex II standard. The ashes used in this comparison were 21, 26, 63, 74, 75. Open points- AAS, closed points, SDS.

A fundamentally more appealing comparison of the surfactants involves showing actual molar uptake at the endpoint. This comparison is shown for SDS, AAS and DBS in Figure 4.4. The DBS solution was initially prepared at 0.025 M concentration. The molar uptake of AAS at the foam endpoint is over five times greater than the molar uptake of SDS, but the different surfactants are clearly well correlated with one another. The molar uptakes of SDS and DBS are much closer to one another at the endpoint. It should be kept in mind what the endpoints actually mean. They are not true equilibrium values, though it would be expected that they should be related to equilibrium uptakes. Also, the endpoint is a function of the particular foaming efficacy of the surfactant in water. It would be expected that the lower the required aqueous phase concentration at the foam endpoint, the lower the molar uptake of surfactant on the carbon surface.

From the preliminary data above, it appeared as though the DBS might be a good choice for a pure surfactant-based standardized foam index test. Figure 4.5 shows the comparison of the performance of this surfactant against the Darex II data for a larger set of ashes. In this case, the DBS concentration had been reduced to 0.00625 M. There is a very good linear correlation. There,

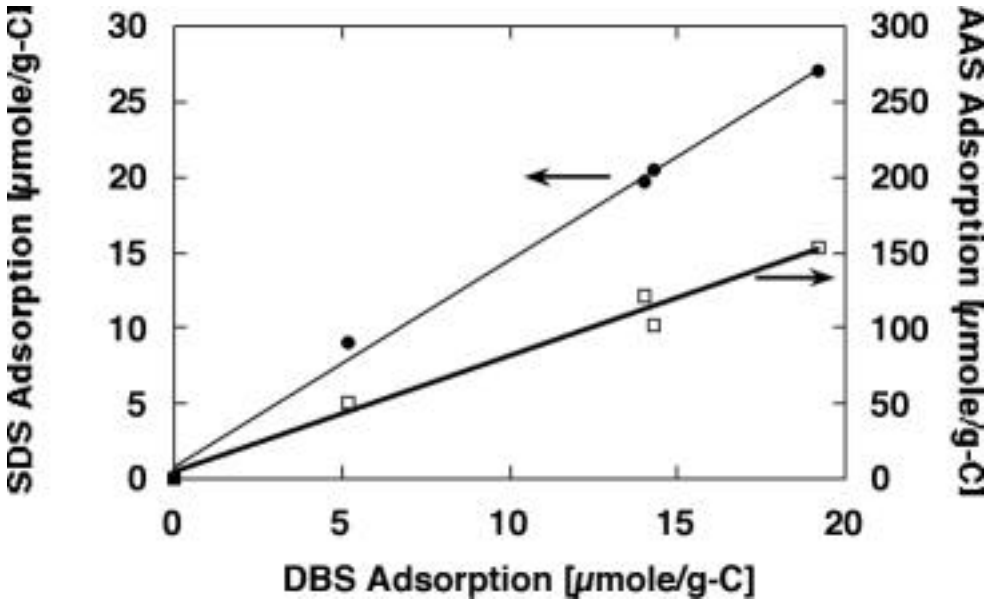

Figure 4.4 Comparison of the relative amounts of adsorption of AAS, SDS and DBS, on a molar basis. The ashes shown are the same as for Fig. 3.

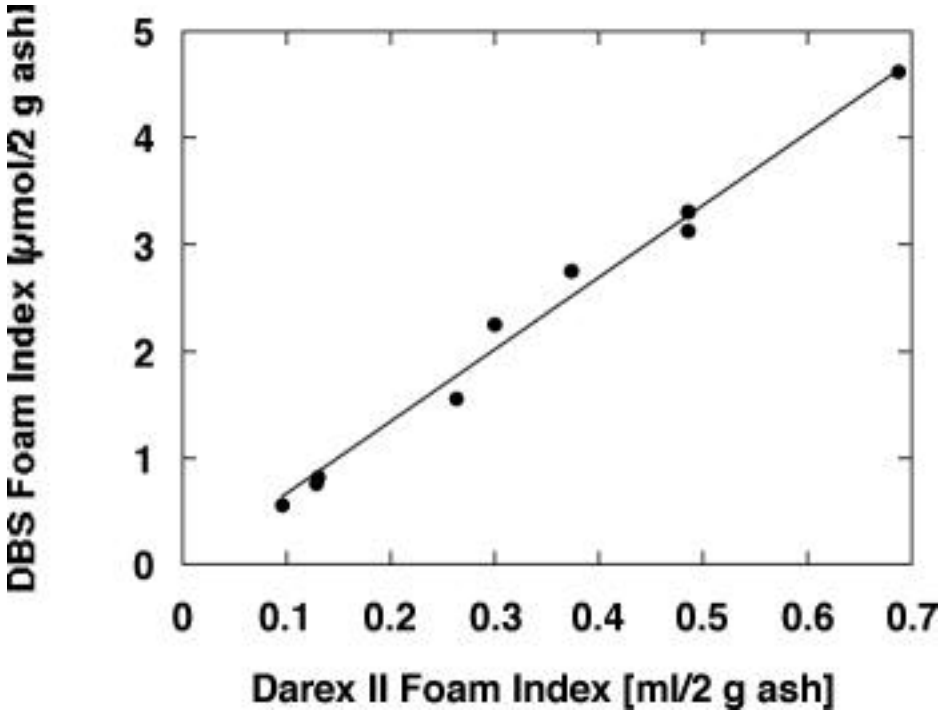

Figure 4.5 Comparison of DBS Foam Index with Darex II foam index, for high LOI ashes. The DBS concentration was 0.00625 M. The ash test set consisted of samples 3, 6, 21, 46, 51, 53, 64, 74, 75.

however, remained a concern that the initial testing had been performed using a set of fly ashes with a biasing towards high LOI values. Consequently, a second round of testing was performed using a set of ashes with much lower LOI values. Because the adsorption capacities of a low LOI set were

much lower, the DBS solution was further diluted to 0.001 M, so as to permit a larger number of drops to be used in determining the endpoint. These results were compared with the results from a series of tests with Darex II solution likewise diluted to 4%, from the normal 10%. The results are shown in Figure 4.6. A reasonable linear correlation is again observed.

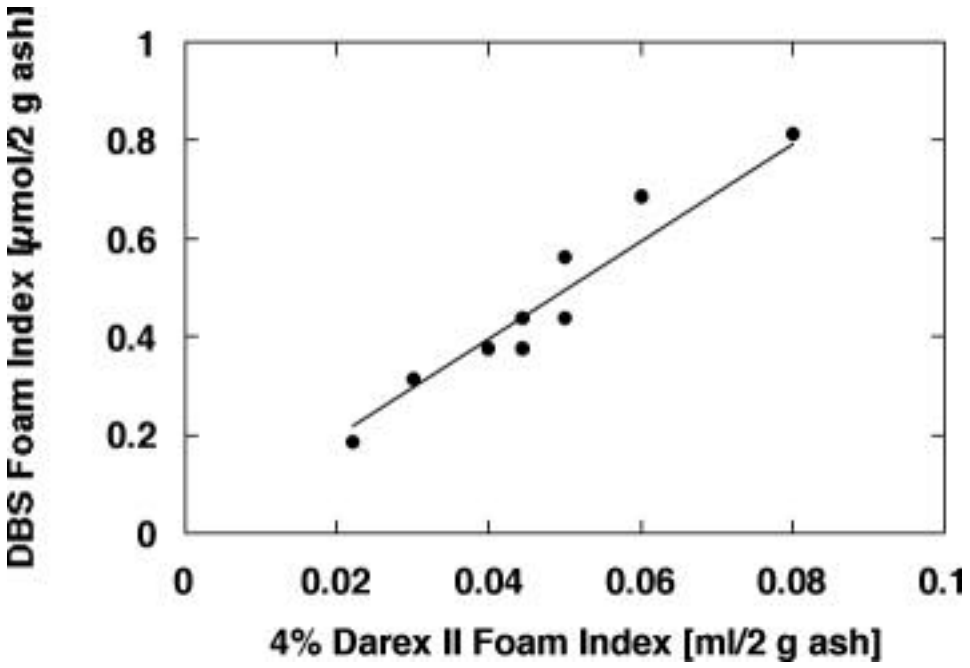

Figure 4.6 Comparison of DBS Foam Index with Darex II foam index, for low LOI ashes. The DBS concentration was 0.001 M. In this test, the Darex II was used in 4% solution. The ash test set consisted of samples 25, 40, 41, 42, 43, 44, 45, 63, 65, 68.

Experiments were also performed with DBS in which the apparent foam index of various salt solutions were explored in the absence of ash and cement, just as they had been with the commercial AEAs. There was somewhat less sensitivity of the results to differences in additives- potassium carbonate added to the deionized water gave foam index results that were similar to those for sodium sulfate or calcium hydroxide. Calcium and sodium carbonate gave only slightly lower effective foam index values than those for the above compounds (differing by only one drop). Calcium chloride again gave unstable foams. These results imply that the use of pure surfactants will tend to make the results of foam index testing somewhat less sensitive to the effects of soluble components in the ash, and to the presence of finely divided calcium solids, than in the case of commercial AEAs.

Surface Capacities of the Fly Ash Carbons

The nitrogen BET surface areas for the ashes tested in this study are shown in Table 4.1. The equivalent surface coverage of DBS on the carbons in the ashes may be estimated using the LOI and BET values in Table 4.1. The results are shown in Figure 4.7. The capacities range from roughly 0.05 to 0.35 µmol/m^2, but there is a cluster of low LOI points near 0.1µmol/m^2 whereas many high LOI points fall at around 0.2 µmol/m^2. What this seems to suggest is that the higher surface area in the lower LOI samples is not equally accessible to DBS as is the surface areas in higher LOI

samples. It has already been noted that accessibility issues do play a role in foam index testing, in connection with the effect of time on the results. Surface area, its accessibility, and other factors determining AEA capacity have been more generally discussed elsewhere [3].

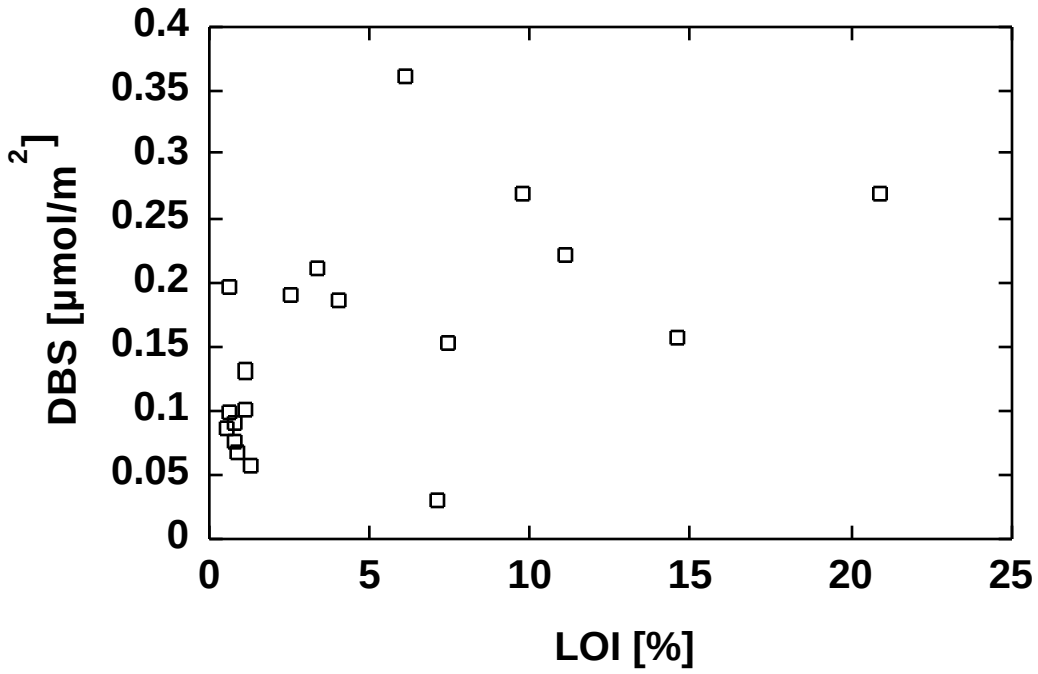

Figure 4.7 Molar uptake of DBS per gram of unburned carbon for the combined sample sets of Figs. 4.5 and 4.6, as a function of unburned carbon content.

As a frame of reference for the above coverage values, it may be noted that a monolayer coverage of nitrogen on carbon would involve roughly 10 µmol/m^2 (using the generally accepted value of 16.2 $Å^2$ for nitrogen [16]). The DBS is a much larger molecule than is N_2, so the fact that the molar capacity for N_2 is higher is not surprising. For example, the surface coverage of pure dodecane has been estimated to be 82.8 $Å^2$ and that of benzene about 43 $Å^2$ [16]. A very crude estimate of surface coverage for DBS would be provided by adding together these two values (assuming that the polar sulfate endgroup would not lie upon the nonpolar carbon surface). In the case of 0.2 µmol/m^2 DBS coverage, it can then be estimated that roughly 15% of a monolayer coverage is achieved on the ash carbon at the foam index endpoint. A less than monolayer coverage might be anticipated for several reasons. One reason is that DBS might be subject to carbon porosity accessibility limitations not important to the much smaller N_2. Of course, the BET model is of questionable theoretical validity in highly microporous materials, and thus comparison of the DBS coverage to a BET surface area is only qualitative.

Chapter 4 summary

There appears to be a good possibility of standardizing the widely used foam index through the use of pure surfactant materials. The present study has shown that there is a good correlation between the adsorption behavior of two commercial anionic AEA materials and three pure surfactant compounds. Apart from the advantage of avoiding issues related to uncontrolled and difficult to characterize "aging" of the commercial materials, the use of pure surfactant materials permits the examination of adsorption effects on a more fundamental basis.

We recommend, as a candidate "standard" procedure our technique based upon use of DBS. This method seems to work as a good surrogate for commercial anionic AEA materials, and the results appear to be well correlated with those obtained using common model anionic surfactants. We also recommend performing the test with addition of cement to the test mixture, in order to create solution conditions most closely resembling those in the actual air entrainment application. It needs to be emphasized that the numerical values of foam index so obtained will, as always, have greatest value when they are correlated with actual air content measurements on a similar set of ash-containing concretes.

References for Chapter 4

1. Gao, Y.-M, Shim, H.-S., Hurt, R.H., Suuberg, E.M. and Yang, N.Y.C., Effects of Carbon on Air Entrainment in Fly Ash Concrete: The Role of Soot and Carbon Black, Energy and Fuels, 11 (1997) 457-462.
2. Freeman, E., Gao, Y.-M., Hurt, R.H., Suuberg, E.M., Interactions of Carbon-Containing Fly Ash with Commercial Air-Entraining Admixtures for Concrete, Fuel, 76, (1997) 761-765.
3. Külaots, I., Gao, Y.M., Hurt, R.H., Suuberg, E.M. The Role of Polar Surface and Mesoporosity in Adsorption of Organics by Fly Ash Carbon, ACS Div. Fuel Chem.
Prepr., 43, (1998) 980-984.
4. Gao, Y.M., Külaots, I., Chen, X., Aggarwal, R., Mehta, A., Suuberg, E.M., and Hurt, R.H., Ozonation for the Chemical Modification of Carbon Surfaces in Fly Ash, Fuel, 80,
(2001) 765-768.
5. Manz, O.E., Coal Fly Ash: A Retrospective and Future Look, Fuel, 78 (1999), 133-136.
6. Yu, J., Külaots, I., Sabanegh, N., Gao, Y.-M., Hurt, R.H., Suuberg, E.M., and Mehta, A., Adsorptive and Optical Properties of Fly Ash from Coal and Petroleum Coke-Co-Firing, Energy and Fuels, 14, (2000) 591-596.
7. Baltrus, J.P. and LaCount, R.B. Measurement of Adsorption of Air-Entraining Admixture on
Fly Ash in Concrete and Cement, Cement and Concrete Research, 31, (2001) 819-824.
8. Rixom, M.R. and Mailvaganam, N.P. Chemical Admixtures for Concrete, E. & F.N. Spon,
New York, 1986, pp 95-139.
9. Standard Specification for Fly Ash and Raw or Calcined Natural Pozzolan for Use as a Mineral Admixture in Portland Cement Concrete, ASTM 618, American Society for Testing and Materials, West Coshohocken, PA, 1996.
10. Brown, R.C. and Dykstra, J.. Systematic Errors in the Use of Loss-on-Ignition to Measure Unburned Carbon in Fly Ash, Fuel, 74 (1995) 570-574.
11. Dodson, V.H., Concrete Admixtures, Van Nostrand Reinhold, New York, 1990, pp 136-143.
12. Helmuth, R. , Fly Ash in Cement and Concrete, Portland Cement Association, Skokie, Il,
1986, pp 80-82.
13. Rivera, R., Air Entraining Admixtures in Applications of Admixtures in Concrete, A.M.

Paillere, Ed., E. & F.N. Spon, New York, 1995.
14. Plante, P. and Pigeon, M. Influence of Soluble Alkali Content in Cement on Air Void Stability in the Presence of Superplasticizer, in Admixtures for Concrete- Improvement of Properties, E. Vazquez, Ed., Chapman and Hall, New York, 1990.
15. Bruere, G.M. Air-Entraining Actions of Anionic Surfactants in Portland Cement Pastes, Jl. of Applied Chemistry and Biotechnology, 21 (1971), 61-64.
16. Gregg, S.J., Sing, K.S.W., Adsorption, Surface Area and Porosity, 2nd Edition, Academic Press, New York, 1982.

RECOMMENDATIONS FOR FUTURE WORK

The data and analyses presented in this report point to the need for future work in certain areas. First, the data in chapter 4 highlight the importance of both mineral effects and pH on the commonly used foam index test and make suggestions for the development of a new standard. While the foam index test is widely applied in industry, and is generally seen as a useful indicator of carbon effects, the test procedures vary from one site to another and this has prevented the establishment of a national database on ash quality. The authors recommend that a standard foam index test be formally proposed and a validation and round-robin testing program be initiated to make this test a national standard. More research into the mineral, ion, and pH effects on the foam index should be part of this program.

Secondly, the data in Chapters 1 and 2 suggest a real commercial potential for ash ozonation. Additional data taken under EPRI sponsorship have addressed the effects of post-ozonation grinding (as may occur during the handling and mixing of fly ash and fly ash concrete) and the reaction engineering aspects of ash ozonation (contacting, reaction rates, side reactions etc). The DOE sponsored data presented here, together with the EPRI sponsored information, provide all the necessary laboratory data to begin a scale-up and commercialization activity. Indeed such an activity is planned at the time of this report writing, in the form of an DOE / EPRI / tailored collaboration to build and demonstrate a large scale version of the ash ozonation process to be hosted at the Montour station of PPL generation. This project plans to use special fluidization technology as the contacting scheme and to employ large-scale ozonation equipment supplied by PCI-Wedeco or West Caldwell, N.J. Based on the results of this testing, a full scale first design will be carried out and economic analyses performed to assess the ozonation technology relative to competing technologies for ash beneficiation. The team believes that ozonation has particular benefits for low-carbon, high-activity ash streams such as those arising from the combustion of PRB coals in facilities equipped with low-NOx burners. No other ash beneficiation process is currently able to handle such low-carbon, high-activity ash streams economically.

Finally, there is a great opportunity to apply the same ozone/carbon surface chemistry for the treatment of activated carbon-based sorbents used in mercury capture. The activated carbon can be treated as part of the ash stream as is the case with native unburned carbon. Of course it is also possible to treat activated carbon before its injection as a mercury sorbent, which greatly reduces the volume of material that must be handled in the ozonation process. For this second option, more work is needed to asses the effects of ozonation on the mercury capture effectiveness of the sorbents. Carbon / Hg chemistry is complex, and ozonation could enhance or degrade the Hg-capture ability of the carbon depending on the conditions and dominant mechanisms. The authors recommend that that the facilities being developed for the ozonation demonstration project be also used for large-scale ozonation of carbon-based Hg-sorbents to provide enough material for duct injection testing under realistic conditions.